October 2015

Measuring Polydimethylsiloxane (PDMS) Mechanical Properties Using Flat Punch Nanoindentation Focusing on Obtaining Full Contact

Federico De Paoli
University of South Florida, depaoli@mail.usf.edu

Measuring Polydimethylsiloxane (PDMS) Mechanical Properties Using Flat Punch Nanoindentation Focusing on Obtaining Full Contact

by

Federico De Paoli

A thesis submitted in partial fulfillment
of the requirements for the degree of
Master of Science in Mechanical Engineering
Department of Mechanical Engineering
College of Engineering
University of South Florida

Major Professor: Alex A. Volinsky, Ph.D.
Nathan Gallant, Ph.D.
Rasim Guldiken, Ph.D.

Date of Approval:
October 19, 2015

Keywords: Polymer, Indentation, Viscoelastic, Cylindrical Punch, Viscosity

DEDICATION

I would like to dedicate this manuscript to my parents and to my sister. Thank you for all your support and encouragement throughout the years.

A heartfelt thanks goes out to my girlfriend Ilaria for all the support and patience shown while I was far (and even while I was at home).

I would also like to thank my friends that are spread around the world and that have always supported me.

ACKNOWLEDGMENTS

I would like to thank my advisor Dr. Volinsky. Without his guidance, this thesis could not be published. I would also like to thank my thesis committee members, Professor Rasim Guldiken and Professor Nathan Gallant for their direction, dedication, and invaluable advice along this project.

I also want to thank the doctorate candidate Asma Sharfeddin for providing valuable help in the laboratory for the production of the samples used in this research work and thesis.

TABLE OF CONTENTS

LIST OF TABLES

LIST OF FIGURES

ABSTRACT

In this research, the materials used were the Polydimethylsiloxane (PDMS) polymers. PDMS mechanicals properties were measured using a customized version of the nanoindentation test using a flat punch tip. The method is proposed in Chapter 3 and it is used to calculate the elastic modulus of different PDMS samples. The samples tested were both produced specifically for this research and available in the laboratory's storage. They all present different levels of cross-linking degree.

It is quite common to not have full contact between the cylindrical flat punch and the sample because of the unavoidable tilt. The new method guarantees establishing full contact between the sample and the tip. The tip used for this purpose is a flat punch tip. The Young's moduli of the following samples were calculated: 10:1, 30:1 and 50:1. The Young's moduli found were: 2.85±0.001 MPa for the 10:1 sample, 0.34±0.001 MPa for the 30:1 sample and 0.15±0.002 MPa for the 50:1 sample. All the experiments were repeated at least three times to assure the validity and the repeatability of the method. The results were then compared with values available in the literature.

The same method was applied to analyze the viscosity of the samples. Even if a mathematical result was not obtained, data and analysis through graphical representations are available in this thesis. The sample tested was a PDMS sample with a cross-linking degree of 30:1. The experiment has been repeated three times

CHAPTER 1: INTRODUCTION

1.1 Introduction to PDMS and its Properties

The material used in this research project is Polydimethylsiloxane (PDMS). It is a mineral-organic silicon-based polymer of the siloxane family [1],[2]. It is also known as Dimethicone and contains silicon, oxygen, and carbon [1].

In the last decade, the interest towards these kinds of materials has increased since they can be used in many different applications. The qualities that make it useful are its elastomeric properties, gas permeability, optical transparency, ease of bonding to itself and to glass, ease of molding, and relatively high chemical resistivity. In addition to those properties, the fact that it is inexpensive to be manufactured makes it noteworthy [3]. PDMS is considered inert, non-toxic and non-flammable [4]. Also, PDMS is biocompatible, so it is appropriate to be used for prosthesis and internal body applications [5]. PDMS has qualities that can be intermediate between an organic and an inorganic material.

The PDMS molecules are highly flexible and they are arranged to form an amorphous material [6]. PDMS, such as the majority of polymers, forms amorphous solids because the process of crystallization is influenced by the topological constraints, such as the crosslinking, and by the difference length of the chains [7].

According to the molecular weight of the samples produced, PDMS presents a low volatility if the molecular weight is high and vice versa [8].

Following is a list of additional properties of the Polydimethylsiloxane that make it noteworthy and useful. PDMS have a low surface tension, a moderate water interfacial tension and no surface viscosity. They can be found in a wide variety of configurations and they present a low activation energy for the viscous flow. In addition to that, PDMS have low glass transition temperature, low boiling points (oligomers), low freezing and pour point and high compressibility. In the environment, they present a low level of hazard, also because of the low flammability, and they are well resistant to the weather. PDMS show high permeability to gas and low molecular weight and a large free volume [9]. Some of the properties described before are only valid for polymer solution, while others are applicable only for chemical cross-linked gels.

Hereafter, the empirical, the chemical and the structural formula of the PDMS will be presented. The empirical formula shows the simplest number ratio of atoms of the elements presents in the compound. Instead, the chemical formula shows how many atoms of each element are present in the compound. With the structural formula, instead, the structure of the molecule is shown.

The empirical formula of the Dimethicone or PDMS is:

$$(C_2H_6OSi)_n \tag{1}$$

The value of n can influence the state of the PDMS. If n, the number of times that the monomer is repeated, is low; then the PDMS will be liquid. If n is high, it will be semi-solid [9],[10].

The chemical formula of the Polydimethylsiloxane instead is:

$$(H_3C)_3\,SiO[Si(CH_3)_2O]nSi(CH_3)_3. \tag{2}$$

The structural formula of the PDMS is shown in Figure 1.

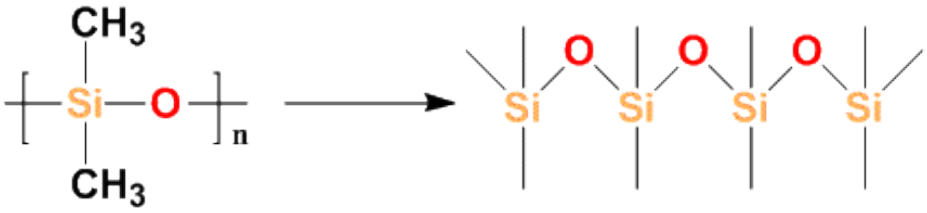

Figure 1. Chemical structure of PDMS [11].

Since it is a polymer, in the structure, there will be a monomer unit ($[SiO(CH_3)_2]$) repeated n-times [2].

A 3D model of the fundamental chemical structure of a Polydimethylsiloxane molecule is shown in Figure 2.

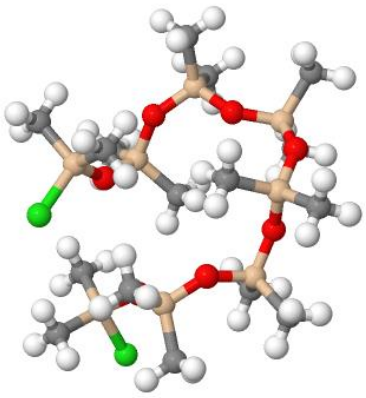

Figure 2. 3D structure of a PDMS molecule [11].

Polymers such as the Polydimethylsiloxane have characteristics halfway between solid and liquid materials. The complexity in measuring their properties comes from their unique texture and consistency. In particular, the consistency of this semi-solid, sticky and viscous material makes it challenging to measure its properties. It is possible to measure them with a macroscopic or microscopic approach. In this thesis, only the microscopic one is used. This research work focuses, in particular, on the use of nanoindentation experiments in order to obtain mechanical properties.

1.2 Applications of PDMS

PDMS, nowadays, is used in many different industries. Those range from the cosmetic industry to the medical field, and from the food making and preservation industry to the production of microfluidic devices [12]. The applications are almost limitless. The following list presents some of the most common uses [8]:

- release agents, adhesives;
- rubber molds, sealants, and gaskets;
- surfactants, water repellents, foam control agents;
- biomedical devices, personal care, and cosmetics;
- dielectric encapsulation, glass sizing agents;
- greases, hydraulic fluids, heat transfer fluids;
- lubricants;
- fuser oil;
- masonry protectants and process aids.

One of the uses, which this research focuses on, is how to use PDMS and its properties to create a substrate to attach and grow cells.

Polydimethylsiloxane has been used in different medical implants and biomedical devices thanks to its biocompatibility and low toxicity. According to Ng Lee et al., the growth rate and quality of the cells, depend on the Young's modulus of the substrate (independent if 0.6 MPa < E < 2.6 MPa) [13]. For this reason and many more, there is a need to develop a method to study the mechanical properties of the material.

The non-toxicity and biocompatibility of this material also explain why it was chosen for the production of breast implants. PDMS is not only used for the production of the silicone gel contained in the implants, but it is also used for the rubber shell that will contain the aforementioned gel [14].

Another main application for PDMS is the fabrication and prototyping of microfluidic chips. Those microchips can be fabricated through molding. Some of the devices so far produced include micro reactors, microchips for capillary gel electrophoresis, and hydrophobic vent valves [15].

Even in everyday products it is possible to find PDMS. For example, in many brands of shampoos, Polydimethylsiloxane is used to increase the hair conditioning effect. This happens due to the quaternized nitrogen that bonds to the backbone of the water-soluble polymer [16].

Due to its non-toxicity, PDMS is also used in the food industry, such as, for example, for the production of the food additive E900 used in the process of making wine and edible oil. The task of this additive is to behave as an anti-foaming agent [17].

PDMS is a good foam control agent because of its low surface tension, thermal stability and chemical inertness [18]. Most of all, silicon oils produced with Polydimethylsiloxane can be used in the food industry because they are not orally metabolized, but they get excreted without being processed by the human body.

The use of these defoamers is extremely important because every biomaterial, such as proteins, vitamins, carbohydrates and fats can act as surfactants producing a viscoelastic layer that stabilizes the foam. Therefore, to avoid the formation of these foams that can damage the final product, PDMS products are largely used in this industry.

PDMS can also be used as a release agent for organic adhesives or directly as a pressure sensitive adhesive. This application is possible thanks to some qualities of the material itself, such as the high level of wettability and its viscoelastic behavior that increases the adhesion and cohesive strength [19].

1.3 Research Objectives

The literature available for this topic is still in an early stage, but it has been growing at a fast pace since the interest linked to this kind of material is expanding. The purpose of this research is to develop a method to use nanoindentation to measure the properties of a soft material, such as PDMS. While nanoindentation measurement is widely used with solid materials, such as metals, it is not yet commonly used for soft and sticky materials, such as polymers and Polydimethylsiloxane. To do so, it is necessary to adapt the standard technique to be usable with PDMS materials. The hardware and the software used to execute the indentation test will be the same one used for the hard materials, but the approach to the experiment and the analysis of the results will differ from the standard one.

One of the main purposes of this research is to find out how to use a flat punch indenter to calculate the mechanical properties of PDMS. This study is based on the assumption that even if the contact area between the flat punch and the sample doesn't change with the indentation depth, to obtain meaningful results, it is necessary to obtain full contact before proceeding

further in the analysis of the mechanical properties [20]. The goal of this thesis is to develop a method to avoid the misalignment tilt and, after developing full contact, calculate the stiffness (Young's modulus) and viscoelasticity of multiple PDMS samples.

The two main properties studied in this research are the elasticity and the viscosity. The difficulty in measuring these values comes from the fact that PDMS is an anomalous material. For example, the adhesion effect, caused by the sticky nature of the material, will cause an overestimation of the elastic modulus [21].

One of the factors that creates a main difference between a test conducted on metals and one done on the polymers is the time. The time holds an important role in the experiments. Many of the properties that are important to be calculated are directly related to the time of loading and unloading of the force. While the speed of loading can influence the results, the biggest changes can be seen in the unloading reaction. The rate of unloading can influence the recording of the data because of the viscoelastic behavior of the sample described by a dashpot. In this research, to avoid this issue, the loading section of the load-displacement graph will be used to calculate the elasticity (since the viscosity won't affect the loading reaction), and both the loading and unloading sections to calculate the viscoelastic effect.

1.4 PDMS Samples Description

In this research, two different groups of samples were tested. The two groups differ in the age of the material. The first group includes samples available in the laboratory produced in 2006. The second group, instead, includes samples that were created specifically for this research. It is important to keep in consideration the age of the samples because the existence of an aging process that can affect the mechanical properties of the sample has been proven [22]. However, further studies and analysis of the aging effect are required.

To create a sample, a base and a curing agent are needed. The silicone elastomer kit used in this research to produce the sample is the "Sylgard 184" of the Dow Corning Corporation. The kit includes a silicone elastomer base and a curing agent, as shown in Figure 3.

The Sylgard 184 elastomeric base contains vinyl group while the curing agent contains a catalyst that catalyze the addition of the SiH bond with the vinyl group forming the linkages [23].

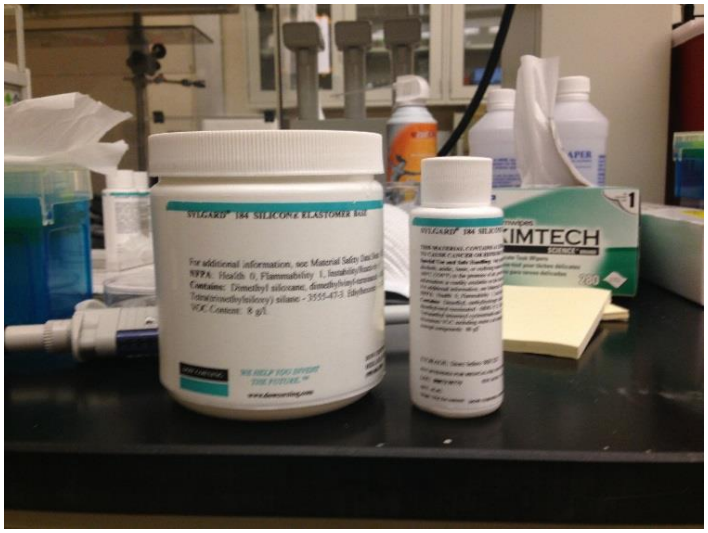

Figure 3. Sylgard 184 silicone elastomer kit.

The samples used have different cross-linking degrees. To produce PDMS with different cross-linking degrees, the ratio between the curing agent and base mixed together is changed. Different cross-linking samples present different stiffness and different mechanical properties [24]. Each sample is labeled with the ratio base:curing agent. For example, some of the samples studied are labeled as 10:1 and 30:1 meaning they have 10 (or 30) masses of Sylgard 184 elastomer base for every mass of Sylgard 184 curing agent. In addition to that, the samples created and used in the experiments have different sizes and thickness. It has been shown that the

mechanical properties depend also on the thickness of the sample [24]. The fact that the elastic modulus and other mechanical properties depend on the thickness of the sample is because of the shear stress during the fabrication of the sample [25].

It is particularly important to keep track of the cross-linking degree of the sample analyzed since the mechanical properties depend directly on it. As shown in the research of Wang et al., the elastic modulus of PDMS can vary from 0.56 MPa to 3.59 MPa according to the cross-linking degree [26]. It is proven that the lower the degree of PDMS network's crosslinking, the softer the material. On the contrary, the higher the degree, the stiffer the PDMS [2].

Table 1. Average stiffness for different cross-linking degree samples [26].

Cross-linking degree	E_{ave} (MPa)
PDMS 5:1	3.59±0.11
PDMS 7:1	2.91±0.036
PDMS 10:1	2.61±0.021
PDMS 16.7:1	1.21±0.069
PDMS 25:1	0.98±0.037
PDMS 33:1	0.56±0.021

Table 1, reported above, shows the results obtained by Wang et al. with a macroscopic compression test. It is important to report these values because they will be compared with the results that will come out from this research. The experiment will involve a microscopic test such as nanoindentation instead of the macroscopic test done by Wang [26].

1.5 PDMS Samples Preparation

Some of the samples used in this research were already available in the storage of the laboratory. However, in order to fully understand the material studied, some new samples were created specifically for this work. In addition to that, it was necessary to have freshly made and

custom-made sample with the cross-linking degree required and the thickness and dimension desired.

To produce a sample, the tools and the materials needed are the following:

- Sylgard 184 silicone elastomer base;
- Sylgard 184 silicone elastomer curing agent;
- Laboratory tools such as Petri dishes and Pasteur pipette;
- Safety tools such as gloves;
- Spoon and cup;
- Scale;
- Vacuum desiccator;
- Oven or hot plate.

The procedure to produce a PDMS sample is described, step by step, in Appendix B.

The process shows how to create a PDMS 10:1 sample. However, it is easily adaptable to create samples with any other cross-linking degree. It is only necessary to change the ratio between the base and the curing agent. The technique to create a PDMS sample is called curing procedure. To cure a PDMS 10:1 sample, 1 gram of silicone curing agent is used for every 10 grams of base. The curing agent and the base need to be mixed homogeneously. To assure that, for a sample 10:1 or 30:1, the mixing time required is around 15 minutes. For a sample with a lower degree of cross-linking, such as 50:1, around 30 minutes of mixing are required.

The curing process can happen in different ways. PDMS can be cured over a wide range of temperatures and times [27]. If it is left at room temperature, the sample will need up to 48 hours to cure completely. If a hot plate or an oven are used, the time decreases exponentially with the increasing temperature.

The only limit on the temperature is given by the limit temperature that a Petri dish can tolerate. With a temperature of 423 K, the time needed is around 10 minutes. The temperature used in this experiment to cure the sample is around 338 K (65 °C) for a time span of 12 hours. Table 2 shows the different ranges of time and temperature that can be used to cure the sample.

Table 2. Time-temperature treatment of PDMS samples [28].

Time	Temperature in °C
10 min	150 °C
20 min	125 °C
35 min	100 °C
48 h	Room temperature (20 °C)

CHAPTER 2: INSTRUMENTATION AND MEASURING METHODS

2.1 Nanoindentation Instrumentation

To conduct the aforementioned experiments, the following tools were used:

- Hysitron TriboIndenter TI900 (Hysitron, USA), shown in Figure 4;
- Flat punch tip with 1002.19 μm diameter;
- A computer with Hysitron TriboScan software (Hysitron, USA);
- KaleidaGraph software for the data analysis and graphical representation.

The TriboIndenter is the hardware machine necessary to perform the indents. The main task of the TriboIndenter is to probe a material surface to nanometer scale depths, while recording the load and depth [29].

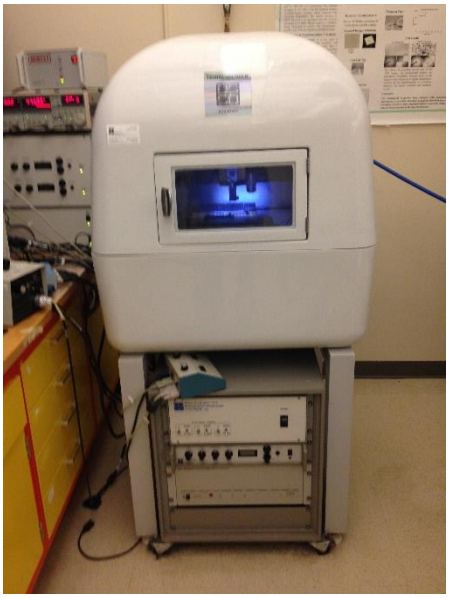

Figure 4. TriboIndenter TI-900.

The part of the instrument that is actually intended to execute the measurement is the three-plate capacitive transducer. The force is applied electrostatically while the displacement is measured by the capacitor. The transducer works by applying an alternating current signal out of phase of 180° to the bottom and top plate. The voltage is then applied to the central plate that is the one allowed to move, causing a displacement. To execute an indent, a direct current voltage is applied to the lower plate of the capacitor and this will cause an attraction between the drive plate and the bottom one, causing the indent [2],[29],[30]. Figure 5 shows a schematic model of the transducer.

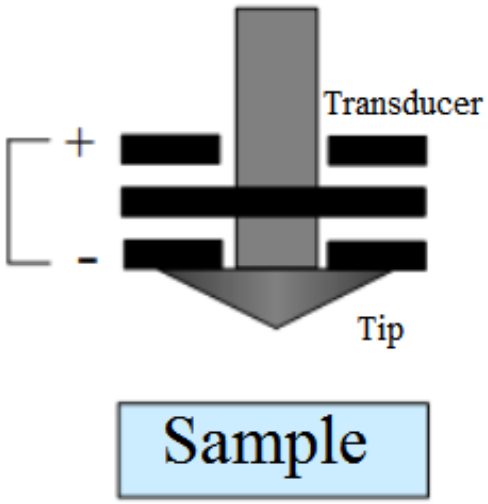

Figure 5. Model of the three plates capacitive transducer of the Nanoindenter [29].

The tip used in this experiment is a flat punch tip that has a cylindrical shape and a diameter of 1002.19 μm. The end of the tip is flat. This kind of tip has been chosen for this research because of the properties of the material tested. Since the sample is extremely soft and sticky, a constant contact area is needed in order to calculate the elastic modulus and any other mechanical properties with satisfying precision. This particular tip is also used when a planar

contact is required. Since the sample and the tip present a tilt, it is necessary to use it to obtain a planar and constant surface of contact [31].

The main software used in this research is the TriboScan whose main window can be seen in Figure 6. It provides complete control over all the Hysitron hardware components and testing experiments [32]. Triboscan was used to set all the parameters needed for the experiment such as the boundaries of the samples and the loading function of the force that includes the time and the peak force value. In addition to that, the TriboScan has the purpose of monitoring and capturing the data that come from the test. The software is also able to analyze and display the results of the indentation [33].

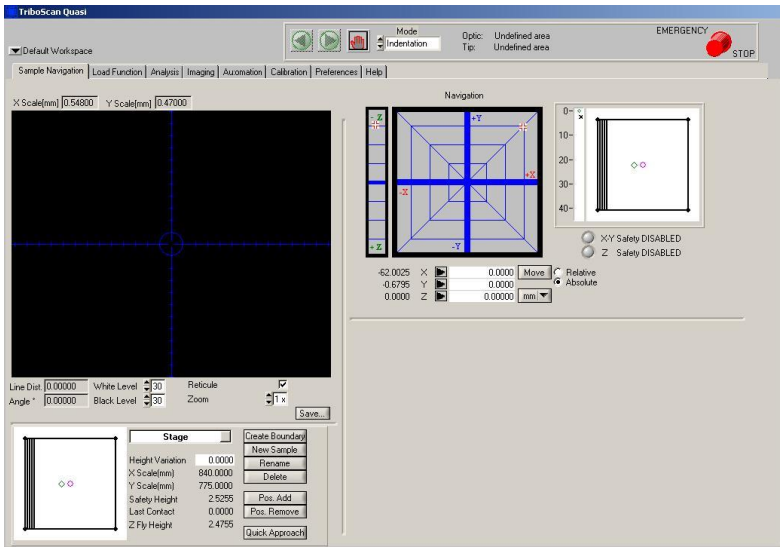

Figure 6. TriboScan main page to set up the indentation parameters and boundaries.

However, even if the TriboScan software can produce graphs of the results, in this research, the plots are created with another software: KaleidaGraph (Synergy Software).

2.2 Governing Equations for Data Analysis

In general, the indentation process is used to calculate the hardness of a specific material. With the improvements in the equipment it is possible to monitor the load and the displacement of the indenter in every instant [34].

One of the most important information needed in order to calculate the mechanical properties desired, after executing an indentation experiment, is the area of the tip used. For the specific tip used in this experiment the residual area is

$$A = \pi \frac{D^2}{4} = \pi \frac{(1002.19)^2}{4} = 788841.97\ \mu m^2 = 0.788\ mm^2 \quad (3)$$

One of the main goals of this research is to develop a method to find the elastic modulus of PDMS. To do so, one of the most important formulas is the one used to calculate the Young's modulus [35]:

$$E_r = \frac{S}{2\beta}\frac{\sqrt{\pi}}{\sqrt{A}} \quad (4)$$

where E_r is the reduced elastic modulus, S is the measured stiffness and A is the contact area of the tip. The constant β depends on the shape of the indenter. For a flat punch tip, the value can be considered equal to 1. For the tip used, the equation can be reduced to [2]:

$$E_r = \frac{S}{2*1}\frac{\sqrt{\pi}}{\sqrt{A}} = \frac{S}{2}\frac{\sqrt{\pi}}{\sqrt{\frac{D^2\pi}{4}}} = \frac{S}{2}\frac{\sqrt{\pi}}{\frac{D}{2}\sqrt{\pi}} = \frac{S}{D} = \frac{S}{1002.19} \quad (5)$$

To calculate the stiffness, there are different possibilities. The one used in this research involves the loading section of the indentation graph. In this graph, the load vs displacement are recorded point by point. As defined, the stiffness of a material is the force (F) per unit of deflection (δ) [35],[36].

$$S = \frac{dF}{d\delta} \quad (6)$$

Since the stiffness is the relationship between the load force and the displacement, it can be calculated using the slope of the loading section of the load-displacement graph. Since the slope is not linear it will be necessary to define an average value of stiffness that will represent the average slope over the displacement range. It can be evaluated using a fitting equation curve. In this case, a linear fit has been chosen and it will return an equation in the form:

$$y = mx + b \tag{7}$$

where m is the slope of the line.

Once the reduced modulus has been calculated, knowing the Young's modulus and Poisson's ratio of the indenter material (respectively E_i and ν_i), it is possible to go back to the Young's modulus [35]:

$$\frac{1}{E_r} = \frac{(1-\nu^2)}{E} + \frac{(1-\nu_i{}^2)}{E_i} \tag{8}$$

For the Poisson's ratio of the indenter (diamond) the value (0.07) has been used and (1140 GPa) as its elastic modulus [20]. It is then possible to obtain the value (0.5) as the Poisson's ratio for the Polydimethylsiloxane from a Polymer Data Handbook [37]. Substituting these values in the previous equation, the relation between the reduced modulus and the Young's modulus of the PDMS is:

$$\frac{1}{E_r} = \frac{(1-0.5^2)}{E} + \frac{(1-0.07^2)}{1140} = \frac{0.75}{E} + 8.72\ X\ 10^{-4} \tag{9}$$

Then, since the second term is negligible:

$$E = 0.75E_r \tag{10}$$

The Young's modulus of a PDMS sample is approximately equal to the 75% of the reduced modulus.

2.3 Polymers Response Models

The behavior of a nanoindenter can be schematically represented as a series of springs [38]. However, for the kind of material studied in this research, this model is not adequate because it doesn't consider the viscoelastic properties.

The two models used to describe more accurately the physics behind the nanoindentation are the Kelvin-Voigt model and the Maxwell one. Hereafter the two models will be described and the fundamental equations will be analyzed.

The Voigt model, schematically represented in Figure 7, consists of a spring and a dashpot connected in parallel. It is used, primarily, to study load control problems such as the creep relaxation [39]. This model is used to analyze viscoelastic solids. An analogy with an electrical circuit can be drawn to solve the fundamental equation.

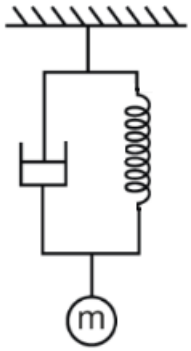

Figure 7. Voigt model (spring and dashpot in parallel) [39].

As it is for the total resistance when there are two resistors in parallel, the same applies for the total force in this case. The total force is then equal to the sum of the force due to the elastic spring and the one due to the damper [40].

$$F = F_s + F_d \tag{11}$$

The Maxwell model instead can be represented as a spring and a damper connected in series. This model, shown in Figure 8, is used for stress relaxation analysis [39]. Another analogy can be drawn with an electrical circuit to calculate the final force.

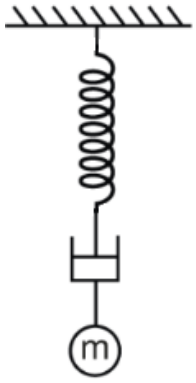

Figure 8. Maxwell model (spring and dashpot connected in series) [39].

The inverse of the equivalent force is equal to the algebraic sum of the inverses of the spring force and the damping force.

$$\frac{1}{F} = \frac{1}{F_s} + \frac{1}{F_d} \tag{12}$$

Those models are quite simplistic and they don't represent the complexity of the real PDMS behavior. To do so, it is necessary to create a combined Voigt and Maxwell model. This model is called Voigt-Kelvin and consists of multiple Voigt modules connected in series. The representation of this model is shown in Figure 9.

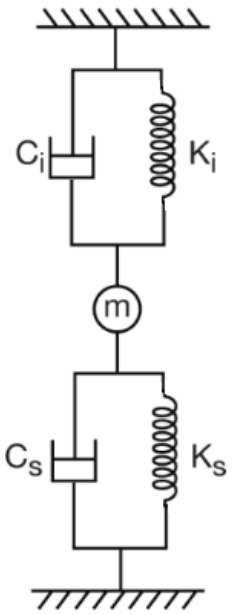

Figure 9. Voigt-Kelvin model [39].

However, even the Voigt-Kelvin model is not enough. The closest model that has been created so far is the Kelvin-Voigt generalized model with quadratic elements shown in Figure 10 below [41].

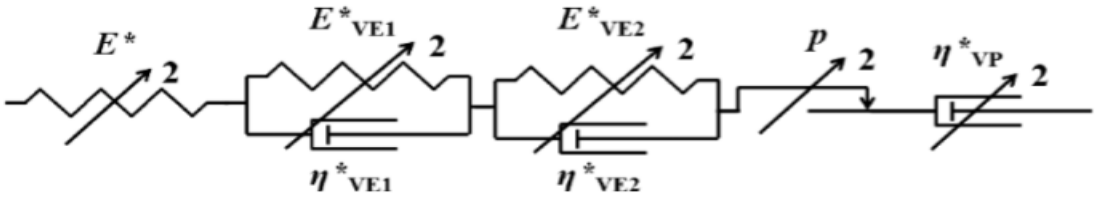

Figure 10. Kelvin-Voigt generalized model with quadratic elements [41].

The model is composed of a series of elements that are used to study and simulate each one of the different characteristics of a PDMS sample. The first element is a spring to describe the elastic behavior, followed by two Kelvin-Voigt elements for the viscoelasticity, followed by a slider for the plasticity and finally a dashpot for the viscoplasticity.

A simplified version of this model is the standard linear solid (SLS) model. The model is composed of one spring placed in series with a Kelvin-Voigt module. The spring is instantaneously activated during loading and it reacts during the unloading with a time dependent response due to the load transfer through the spring-dashpot [42].

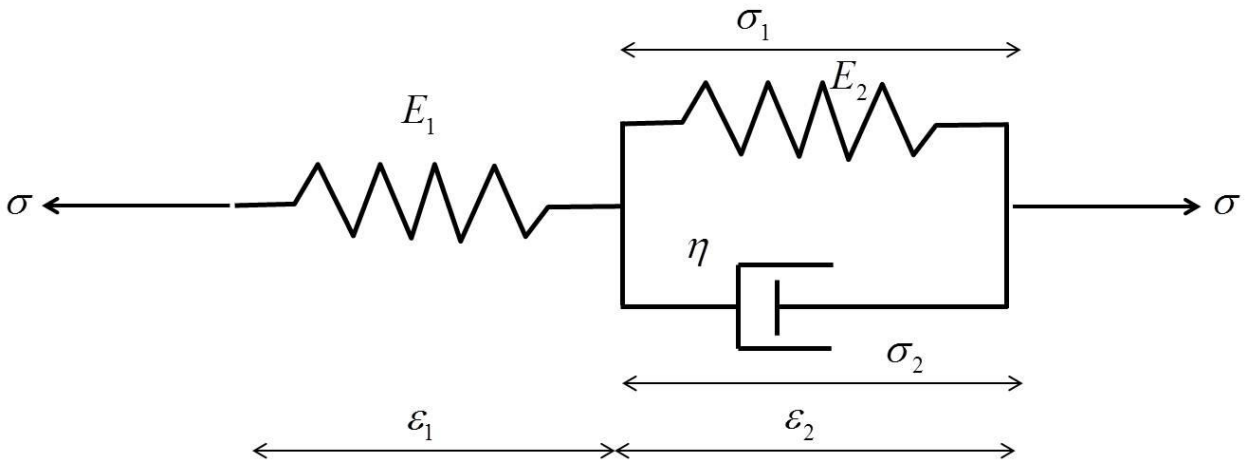

Figure 11. Standard linear solid model [42].

CHAPTER 3: EXPERIMENT TO CALCULATE THE YOUNG'S MODULUS [1]

3.1 Purpose and Differences From Previous Experiments

The first experiment conducted was for developing a method to calculate the Young's modulus of a PDMS sample. Before being able to calculate the mechanical properties of a sample using nanoindentation, full contact between the tip and the surface needs to be established. Before proceeding further with the analysis of the results obtained from the indentation, it is necessary to describe the procedure to establish full contact between the sample and the 1002.19 μm diameter cylindrical flat punch.

This procedure differs from the standard automated indentation because each indent has to be performed manually after establishing full contact with the sample surface. Incomplete contact happens because of the sample tilt with respect to the flat punch surface, and results in incorrect values of the desired mechanical properties measured. Thus, it is then impossible to use the automated indentation. Using the standard procedure will provide incorrect values due to initial incomplete contact.

After reaching full contact, it will be possible to proceed to calculate the mechanical properties desired. In particular, for this research, the elastic modulus (Young's modulus) will be calculated. Another difference from the standard procedure is that, to calculate the elastic modulus of the sample, the loading portion of the slope will be used since the unloading one is affected by viscoelastic deformation.

[1] Portions of this chapter were previously published in [44].

Every sample tested is described with the acronym PDMS, followed by the elastomer base/curing agent ratio. For example, the first sample studied is named PDMS 10:1, meaning that the base/agent ratio is 10, with 10 mass units of the silicone elastomer base mixed with 1 mass unit of the silicone elastomer curing agent.

In this research, the samples studied are multiple and they present the following cross-linking degrees: 10:1, 30:1, 50:1.

3.2 Obtaining Full Contact

In order to calculate the desired mechanical property, it is necessary to know the contact area between the tip and the sample. The surface area of the tip in this report is equal to 0.788 mm^2. This area doesn't change during a flat punch indentation.

However, the full contact between the flat punch tip and the sample is not initially established due to the unavoidable sample tilt with respect to the cylindrical flat punch surface, which results in incorrect elastic modulus values when using automated indentation [43]. This situation is shown schematically in Figure 12. The angle of tilt between the tip and the sample is unknown.

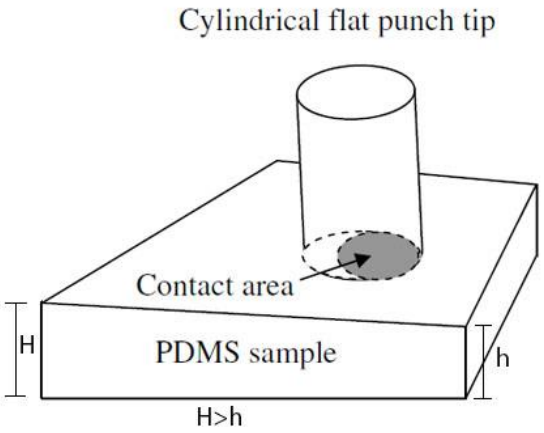

Figure 12. The schematic tilt between flat punch tip and sample [44].

The hypothesis behind this research, is that full contact can be achieved by moving the tip into the sample in 2 μm increments, up to 50-60 μm maximum combined displacement, until the loading stiffness no longer increases. The 2 μm threshold has been arbitrarily chosen because it is small enough. However, it is possible to substitute this value with similar small values.

To start the procedure, it is necessary to first set up the Hysitron TriboIndenter and the TriboScan software. The machine needs to be calibrated, which is achieved following the standard air indentation procedure [45]. It is possible to consult in Appendix A the setup values and procedure used. The air indentation is performed to calibrate the transducer electrostatic force and check the transducer plates spacing [26]. This is the only step that resembles the so-called "standard" indentation test. The rest of the procedure is different from the standard procedure. The Figure 13 below shows the results obtained from the air calibration of the TriboIndenter.

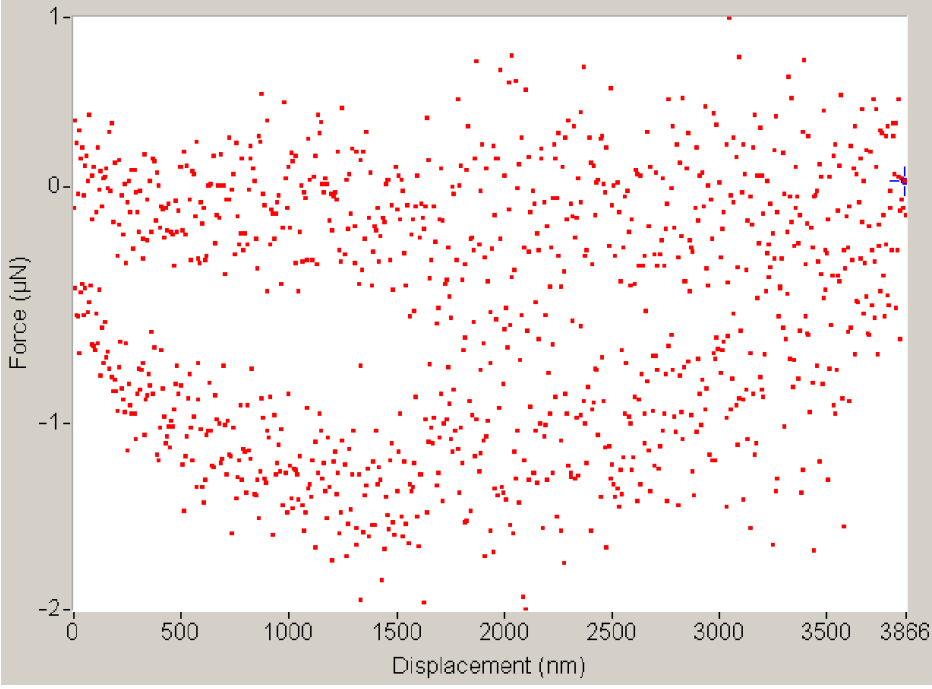

Figure 13. Air calibration (force-displacement).

The experiment consists of moving the tip deeper into the sample surface in 1-2 μm increments relative to the previous position by manually raising the sample stage. The relative sample stage movement increment is chosen as 1-2 μm, or higher each time, based on the maximum displacement reached in the previous indent at the pre-defined 600 μN maximum load. Figure 14 shows the setup values for the air indentation calibration.

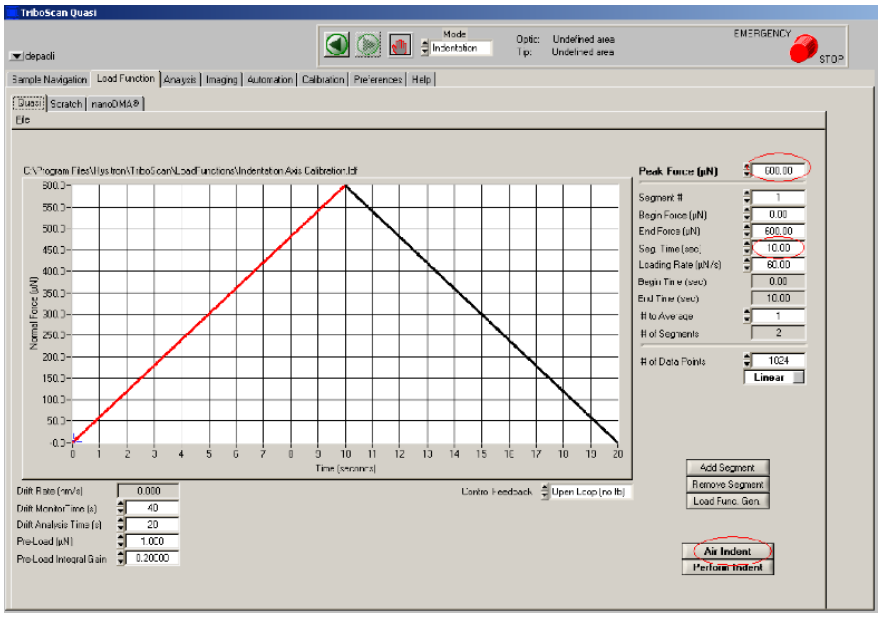

Figure 14. Initial setup of the TriboScan software.

Attention should be paid not to exceed the total displacement above 60-70 μm. This limitation is due to the spacing between the transducer capacitor plates of around 80-100 μm. Assuming that the initial position is at the center of the available displacement range, it is safe to keep the total stage movement under 60-70 μm. The total allowable displacement also depends on the sample stiffness, and it is safe to have up to 80 μm maximum displacement for the softer PDMS samples. This limit can be set at 60-70 μm of total relative movement for safety reasons. However, even if the plate is moved by 70 μm, the total displacement will be smaller than that. In fact, the plate would actually move 70 μm only if an air indentation would be made.

However, since the tip is in contact with the sample, the total displacement moved is actually smaller. Still, it is better to maintain 70 μm as the maximum limit. Sample safety boundaries do not need to be defined using this modified testing procedure.

Before starting the test, the tip is moved manually, using the stage, above the sample surface and lowered to make the first contact with the PDMS sample. The problem with this kind of material is that, even if the tip is in contact with the sample, there is no guarantee that it is in full contact, since the sample surface is always tilted with respect to the flat punch tip surface, as shown schematically in Figure 12. Before collecting any meaningful indentation data, full contact between the tip and the sample surface must be established. If the full contact is not established, erroneous modulus will result.

The tip has to be moved deeper into the sample until the measured stiffness of the sample won't change with a further increase of the relative indentation depth. The load function, chosen for this experiment, is shown in Figure 15.

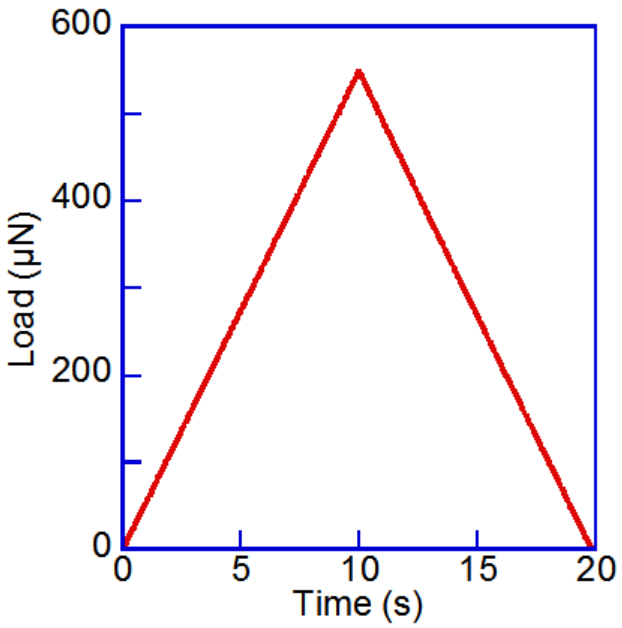

Figure 15. Load function (load-time curve) of the indentations conducted (PDMS 10:1) [44].

As it can be seen in the graph, the peak load value is <600 μN while the loading and the unloading time are 10 seconds each. This typical maximum load is used during the air indentation calibration, which results in about 4-5 μm tip travel range in air, without contacting the sample [45]. The Hysitron TriboIndenter transducer has ~5 μm maximum travel range, thus, the selected 600 μN maximum load will not result in exceeding the maximum transducer displacement. The indents are performed in the open-loop mode, i.e. pseudo-load control.

To ensure the full contact, the first step requires to mount the sample on the stage and define the sample in-plane boundaries in the TriboScan software. Air indentation calibration is performed to make sure that the Hysitron transducer is calibrated and working properly. The sample stage is then moved to position the tip above the sample surface, and then the stage is moved along the vertical Z direction until there is the first contact between the tip and the sample. Exceeding the maximum safety load, which stops the stage motors, can be avoided by pressing the "AUTO ZERO" button on the transducer controller.

At this point, it is possible to perform the first indentation into the PDMS sample. The loading slope graph results that are obtained, are not consistent. It is possible to see how it changes as a function of the relative indentation depth due to incomplete contact between the flat punch tip and the PDMS sample, as shown in Figure 16.

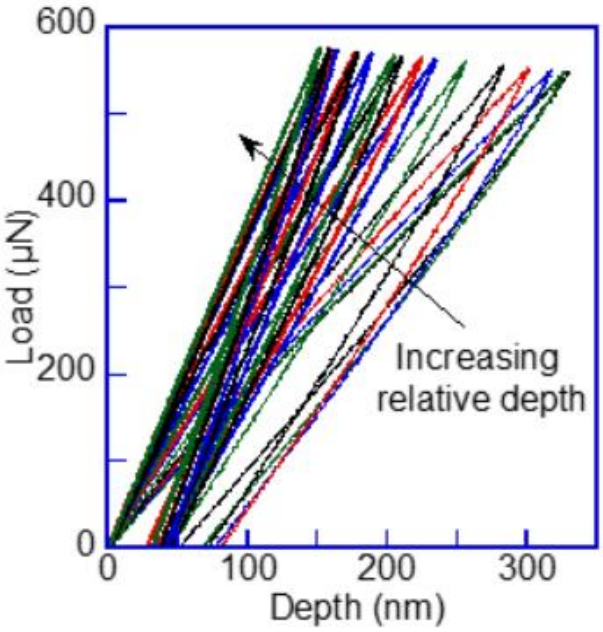

Figure 16. Load-displacement curves showing increasing stiffness with increasing depth (PDMS 10:1) [44].

The sample stage is manually moved up using the Triboscan software controls towards the tip to increase the relative indentation depth in 1-2 μm increments, which results in increased loading stiffness in Figure 17.

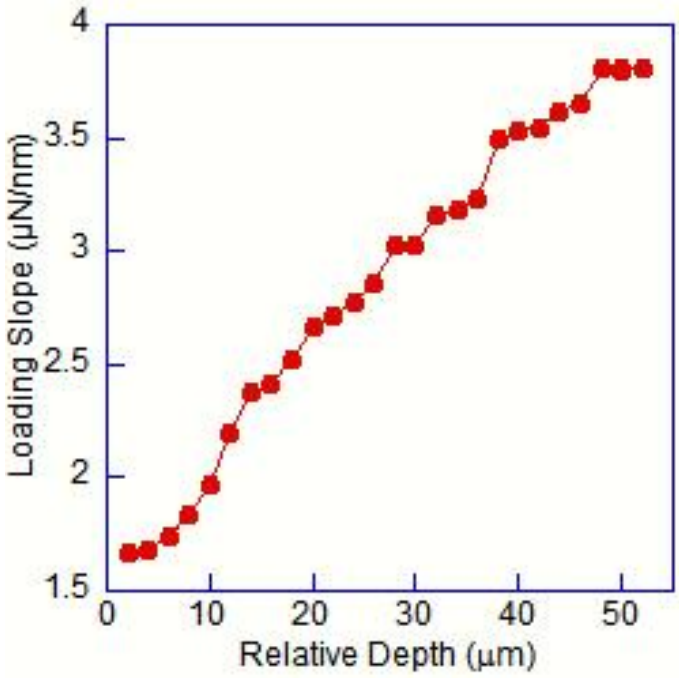

Figure 17. Loading stiffness vs. relative depth (PDMS 10:1) [44].

The stage movement increment is based on the maximum transducer 5 μm displacement range and the maximum indentation depth of the previous indent, which was on the order of 300 nm. This procedure is repeated until the loading slope doesn't increase anymore. In this case, the procedure was repeated 24 times before obtaining a consistent result.

Table 3 shows all the slopes obtained from every single indentation at the corresponding relative depth. It is important to report this table because it shows that the values of the slope keep increasing. These data are used to create Figure 17.

Table 3. Data collected showing the relative depth and loading slope (PDMS 10:1).

Relative Depth (μm)	Loading Slope (μN/nm)	Relative Depth (μm)	Loading Slope (μN/nm)
2	1.6676	30	3.0324
4	1.6848	32	3.1581
6	1.7364	34	3.1811
8	1.8406	36	3.2292
10	1.9728	38	3.4933
12	2.2005	40	3.5275
14	2.3773	42	3.5429
16	2.4127	44	3.6191
18	2.5178	46	3.6501
20	2.6669	48	3.8040
22	2.7092	50	3.8040
24	2.7801	52	3.8040
26	2.8568	50	3.7987
28	3.0273		

After moving the sample stage by 48 μm into the indenter tip, there was no further change in the loading stiffness as can be seen in Figure 18 with the stage motion of 50-52 μm. This proves that the full contact between the tip and the PDMS sample is reached. Decreasing the depth by 2 μm also demonstrates that there is full contact since the loading stiffness of the three load-displacement curves is the same in Figure 18.

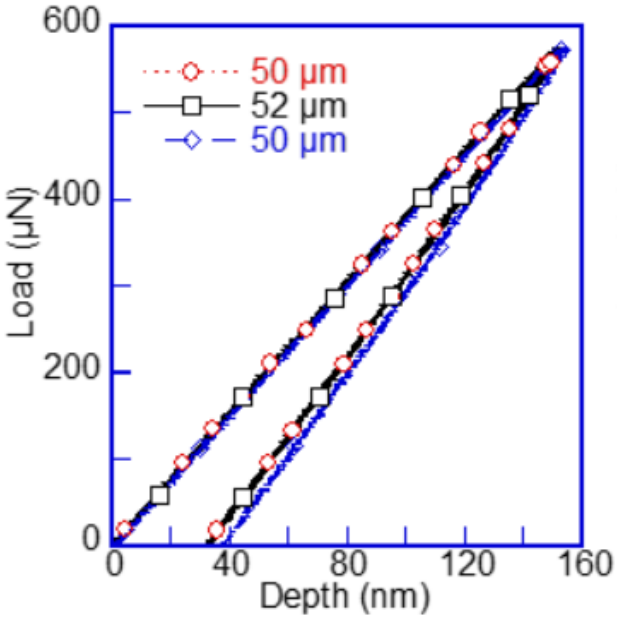

Figure 18. Load-displacement curves after reaching saturation at 50 μm relative tip depth (PDMS 10:1) [44].

In Figure 18, it is clear that even at 50 μm and 52 μm relative displacements there is no change of the loading slope. If the tip is retracted by 2 μm, therefore returning to the 50 μm relative depth, the loading slope remains the same. This proves that the full contact was established. Unchanged loading slope also suggests elastic contact and no plastic deformation of the PDMS sample.

The next step needed to proceed further in calculating the mechanical properties of the sample, is to obtain the equations of the fitting curves. The three equations obtained for the 50 μm, 52 μm, and again 50 μm relative depth indentations are the following:

$$y = 3.8073x + 3.24 \quad (13)$$

$$y = 3.8073x + 3.24 \quad (14)$$

$$y = 3.7743x + 0.01 \quad (15)$$

The slope of the three lines is the same, with a reasonably small uncertainty or error in terms of bias and variance. This difference or error is due to the sensibility and level of precision of the instrument used.

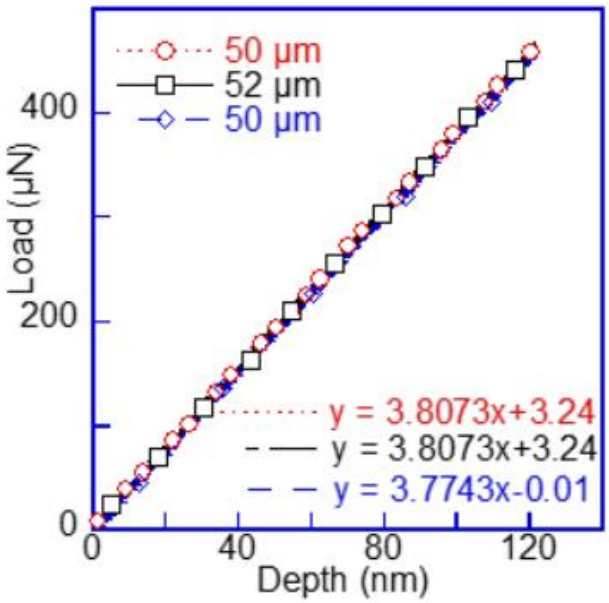

Figure 19. Loading portions of load-displacement curves at 50 and 52 µm relative depth (PDMS 10:1) [44].

Usually, for metals and other ductile materials the unloading slope is used to measure the stiffness and calculate the elastic modulus. This happens because they undergo elastic and plastic deformation during loading, followed by elastic recovery upon the unloading. Viscoelastic soft polymers, such as PDMS, are different, however, since they undergo viscoelastic deformation upon the unloading. This is why the slope during fast loading is utilized in the described method to calculate the elastic properties of soft PDMS. Loading time should be reduced to minimize the effects of viscoelastic deformation during loading.

3.3 Elastic Modulus of a PDMS

The elastic modulus, also known as Young's modulus, can be calculated, for idealistic solid using the Hooke's law.

$$E = \frac{stress}{strain} = \frac{\sigma}{\varepsilon} \tag{16}$$

where E is the Young's modulus, σ is the stress and ε is the strain. The stress and the strain can be both tensile or compressive [2]. Figure 20 represents a typical stress-strain graph and it shows how the Young's modulus is the slope of the line tangent to the curve.

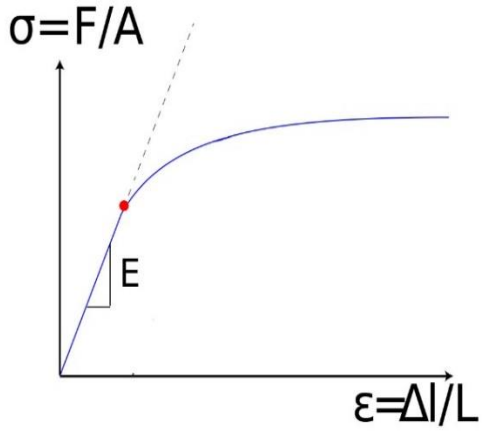

Figure 20. Stress-strain graph. [46]

The stress σ has the units of pressure (GPa, MPa or KPa) since it is a force per unit area while the strain ε is dimensionless. The stress can be caused by compression or by tension. The strain is even called "percentage elongation" since it is the change in the length per unit length [2].

$$\varepsilon = \frac{(L - L_0)}{L_0} \tag{17}$$

where L is the original length and $L_0$is the final length.

From these equations, it is obvious that, if the strain is unvaried, the stiffness of the material increases if the stress is larger. In the SI, then, the Young's modulus has the dimensions of a pressure.

3.4 Elastic Modulus Calculation

After plotting the slope of the full contact, as seen in Figure 19, it is possible to calculate the reduced elastic modulus of the PDMS sample by using the loading slope and the equation (6). Since there is not an exact value for the slope, in this research the average between the slope of the 50 µm, 52 µm, and 50 µm relative depth is used:

$$S_{avg} = \frac{3.8073 + 3.8073 + 3.7743}{3} = 3.7963\ \mu N/nm \tag{18}$$

$$E_r = \frac{S_{avg}}{D} = \frac{S_{avg}}{1002.19} = \frac{3.7963}{1002.19} = 3.7889\ \text{MPa} \pm 0.019\ \text{MPa} \tag{19}$$

Here, S_{avg} is the measured average loading stiffness, and D is the flat punch tip diameter. The reduced elastic modulus of the PDMS 10:1 sample is then 3.8 MPa [20]. The elastic modulus of the PDMS is 25% smaller than the reduced modulus, and it is consistent with previous nanoindentation measurements [20],[47]:

$$E_{PDMS} = 0.75 \cdot E_r = 2.85\ \text{MPa} \tag{20}$$

Metals and other ductile materials undergo elastic and plastic deformation during loading, followed by elastic recovery upon the unloading. This is why the unloading slope is used to measure the stiffness and calculate the elastic modulus of these materials. However, viscoelastic soft polymers are different since they undergo viscoelastic deformation upon the unloading. This is why the slope during fast loading is utilized in this method to calculate the elastic. Loading time should be reduced to minimize the effects of viscoelastic deformation during loading.

This experiment has been conducted on different PDMS samples. The samples tested were: samples of PDMS 10:1 created at different times, samples of PDMS 30:1 and PDMS 50:1. Significantly older samples (over 5 years old) have a higher elastic modulus, demonstrating some aging phenomena. A PDMS 10:1 sample produced in 2006 and tested following this method showed an elastic modulus higher than 7 MPa. However it was not possible to prove if this increment in stiffness was due to the aging effect or because of the sample were damaged or corrupted.

3.5 PDMS Elastic Modulus Results from Different Samples

In the next two subsections the experiment done on a 30:1 and 50:1 PDMS sample are presented. The test was conducted only on one sample of each cross-linking degree. However all the procedures were repeated three times for each sample in order to guarantee the validity of the results.

3.5.1 Indentation of 30:1 PDMS Sample

After conducting the experiment on the sample PDMS 10:1 and having established a method, the same experiment was executed on different samples with different cross-linking degrees. The second sample studied presents a cross-linking degree of 30:1, meaning that there are 30 masses of Sylgard 184 silicone elastomer base for every mass of Sylgard 184 curing agent. The sample used can be seen in Figure 21 below. It is 1 mm thick and it was produced in May 2015. The experiment was conducted in the same month of the manufacturing.

Figure 21. Sample of PDMS 30:1 used in the experiment.

The procedures applied resembles the one used in the previous experiment on the PDMS 10:1 sample. In this chapter, only the results will be presented.

The first graph presented in Figure 22 is the load versus time. This is useful because it shows how the force function is applied to the sample.

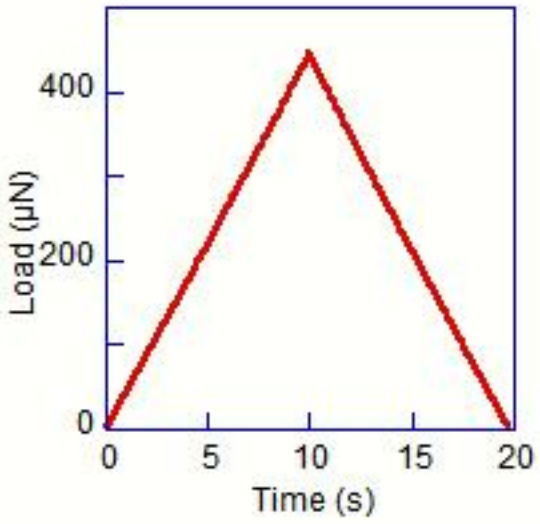

Figure 22. Load function (load-time curve) of the indentations conducted (PDMS 30:1).

The peak load value, in the TriboScan software, is set at 600 µN. However, the peak value reached is lower than 500 µN, while the loading time and the unloading one are both 10 seconds, as seen in Figure 22.

Following the established protocol, it is now necessary to obtain the full contact. In Figure 23, all the executed indentations are shown before reaching the condition of full contact. In this particular experiment, it was necessary to repeat the procedure 51 times in order to obtain the full contact. Since the relative movement is set at 2 µm and since this value is kept constant, the total displacement is equal to 102 µm.

While the tip keeps getting deeper and deeper into the sample, it is shown how the stiffness increases. Having reached the full contact, the stiffness of the sample no longer increased and stabilized around a certain value.

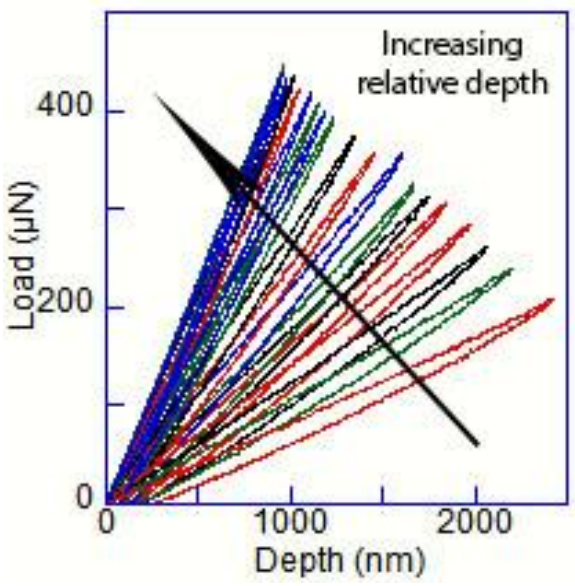

Figure 23. Load-displacement curves showing increasing stiffness with increasing depth (PDMS 30:1).

The plot, shown in Figure 24 represents the relationship between the relative depth and the stiffness and it shows how the slope of the loading section of the graphs keeps increasing until 102 µm of relative depth is reached. At this value, the stiffness stops to increase and it remains constant even if the depth keeps increasing.

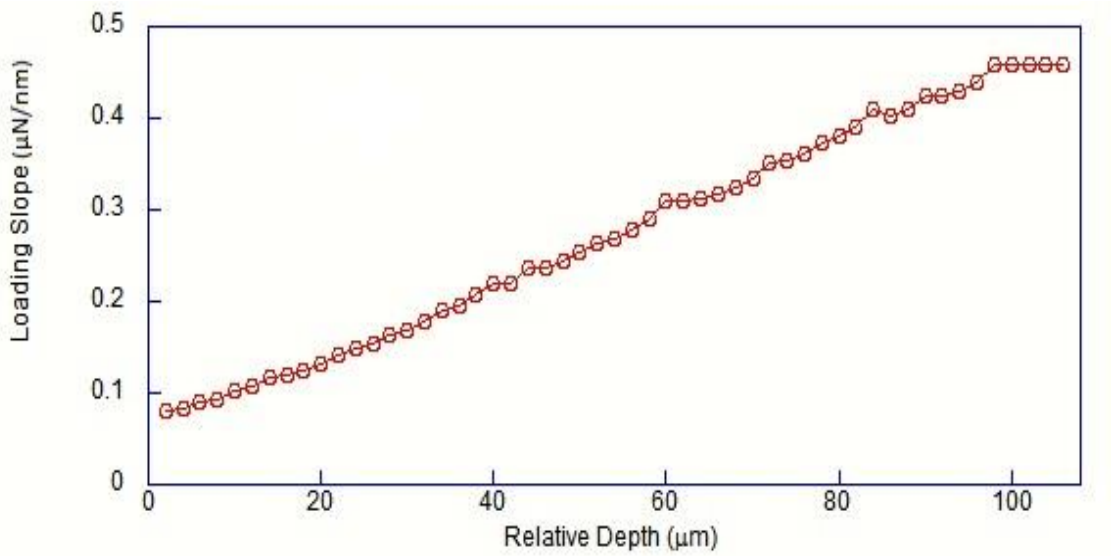

Figure 24. Loading stiffness vs. relative depth (PDMS 30:1).

It can be seen how the full contact is reached when the loading slope stops increasing and a plateau is obtained.

Table 5 shows the values of the stiffness of the loading slope at every relative depth value. These data are necessary to be able to prove that full contact is reached. The values of the loading slope go from 0.080053 µN/nm during the first indentation, up to 0.45852 µN/nm in the 102nd indentation. It is possible to see from Table 4 how the value of the loading slope stabilizes once the full contact is obtained.

Table 4. Data collected showing the relative depth and loading slope (PDMS 30:1).

Relative Depth (µm)	Loading Slope (µN/nm)	Relative Depth (µm)	Loading Slope (µN/nm)
2	0.080053	56	0.27778
4	0.084021	58	0.29091
6	0.090945	60	0.30906
8	0.094003	62	0.31111
10	0.10347	64	0.31214
12	0.10760	66	0.31780
14	0.11644	68	0.32473
16	0.11909	70	0.33472
18	0.12432	72	0.35229
20	0.13252	74	0.35276
22	0.14279	76	0.36215
24	0.15016	78	0.37421
26	0.15425	80	0.37952
28	0.16457	82	0.39040
30	0.16885	84	0.40897
32	0.17873	86	0.40314
34	0.19089	88	0.41056
36	0.19473	90	0.42540
38	0.20666	92	0.42650
40	0.21856	94	0.43057
42	0.21878	96	0.43839
44	0.23569	98	0.45847
46	0.23658	100	0.45850
48	0.24501	102	0.45852
50	0.25272	104	0.45851
52	0.26376	106	0.45848
54	0.26813	104	0.45860

At a relative depth of 98 µm, 100 µm, and 102 µm, the slope doesn't change anymore and it is the proof that full contact is reached. The following graph, in Figure 25, focuses on those indentations done at a relative depth of 98, 100 and 102 µm.

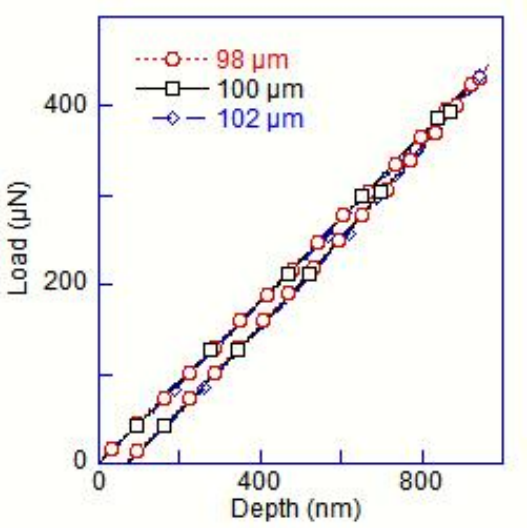

Figure 25. Load-displacement curves after reaching saturation at 100 µm relative tip depth (PDMS 30:1).

Finally, in order to calculate the Young's modulus, it is necessary to extrapolate the fitting equations of the loading sections from the graph in Figure 26.

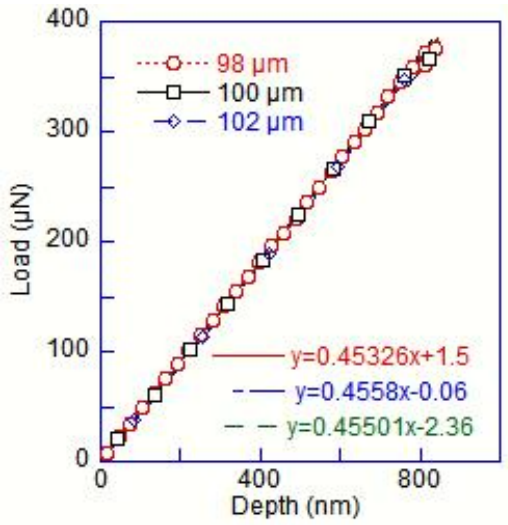

Figure 26. Loading portions of load-displacement curves at 98, 100 and 102 µm relative depth (PDMS 30:1).

The equations of the three lines are the following:

$$y = 0.45326x + 1.5 \tag{21}$$

$$y = 0.4558x - 0.6 \tag{22}$$

$$y = 0.45501x - 2.36 \tag{23}$$

Calculating the average slope yields:

$$S_{avg} = \frac{0.45326 + 0.4558 + 0.45501}{3} = 0.45469 \ \frac{\mu N}{nm} \tag{24}$$

Applying equation (6) the reduced elastic modulus is found:

$$E_r = \frac{0.45469}{1002.19} = 0.4537 \text{ MPa} \pm 0.0013 \text{ MPa} \tag{25}$$

Finally, the elastic modulus can be calculated using the formula (11):

$$E = 0.75 * 0.45 = 0.34 \text{ MPa} \tag{26}$$

The elastic modulus of the PDMS sample with a degree of cross-linking 30:1 is then equal to 0.34 MPa or 340 KPa. This value is considered acceptable and it is of the same order of magnitude of the values calculated with different techniques described in the literature.

For example, in the research conducted by Gupta et al. a value equal to 0.42 MPa was measured [48], while according to Genchi et al., the value is equal to 0.19 MPa [49]. Other results are available in the literature. According to the macroscale tests, conducted by Sharfeddin et al., the elastic modulus for a 30:1 PDMS sample varies from 0.83 MPa if measured with a compression test to 0.17 MPa obtained with a tensile test [50].

3.5.2 Indentation of 50:1 PDMS Sample

The third experiment was conducted on a sample of PDMS 50:1. The low degree of cross-linking cause the sample to be very sticky and with a low Young's modulus. Also for this sample only the results will be presented in this research work. Figure 27 below shows the sample used in this experiment. It presents a thickness of 1 mm. The sample was produced in May 2015, same month during which the experiment was conducted.

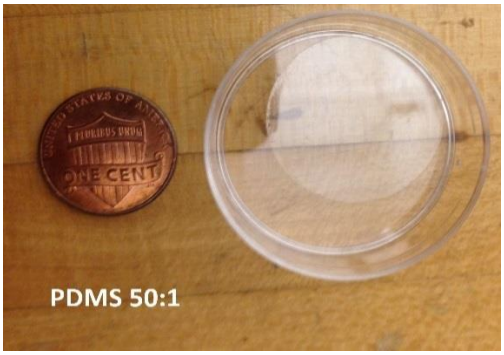

Figure 27. Sample of PDMS 50:1 used in the experiment.

In Figure 28, the time vs load graph is shown. The time of loading and unloading is set at 10 seconds each.

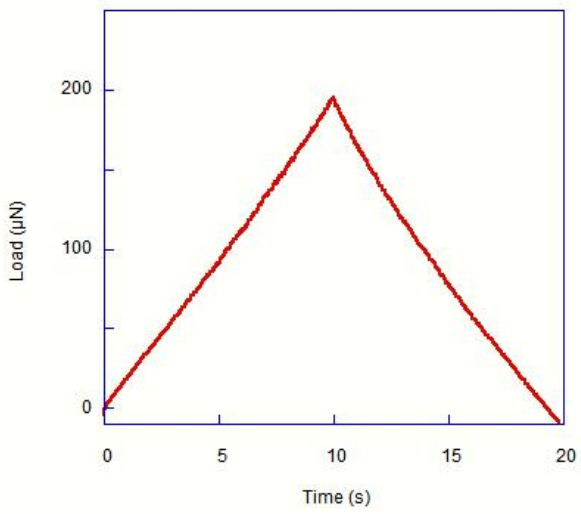

Figure 28. Load function (load-time curve) of the indentations conducted (PDMS 50:1).

The peak value reached is around 200 µN even if the peak value set in the TriboIndenter is equal to 600 µN. This happens because of the nature of the sample. The stiffer the sample, the less deep the tip will go keeping the same load force.

Following the procedure to establish full contact, the graph shown in Figure 29 was obtained. It shows the 45 indentations were necessary to obtain the full contact.

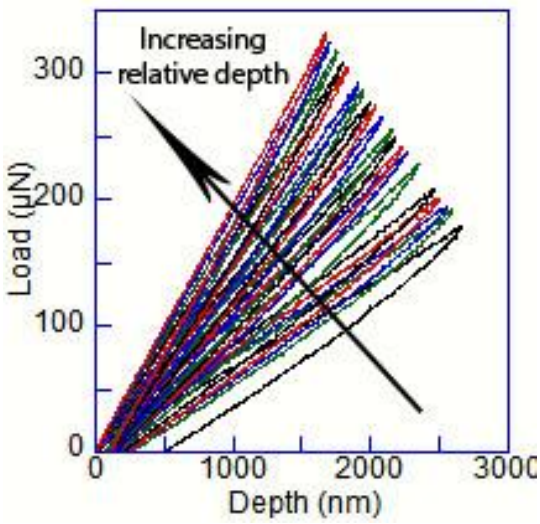

Figure 29. Load-displacement curves showing increasing stiffness with increasing depth (PDMS 50:1).

The plot, shown in Figure 30, that represents the relationship between the relative depth and the stiffness will show how the slope of the loading section of the graphs keeps increasing until 88 µm of relative depth is reached. At this value, the stiffness stops to increase and remains constant even if the depth keeps increasing.

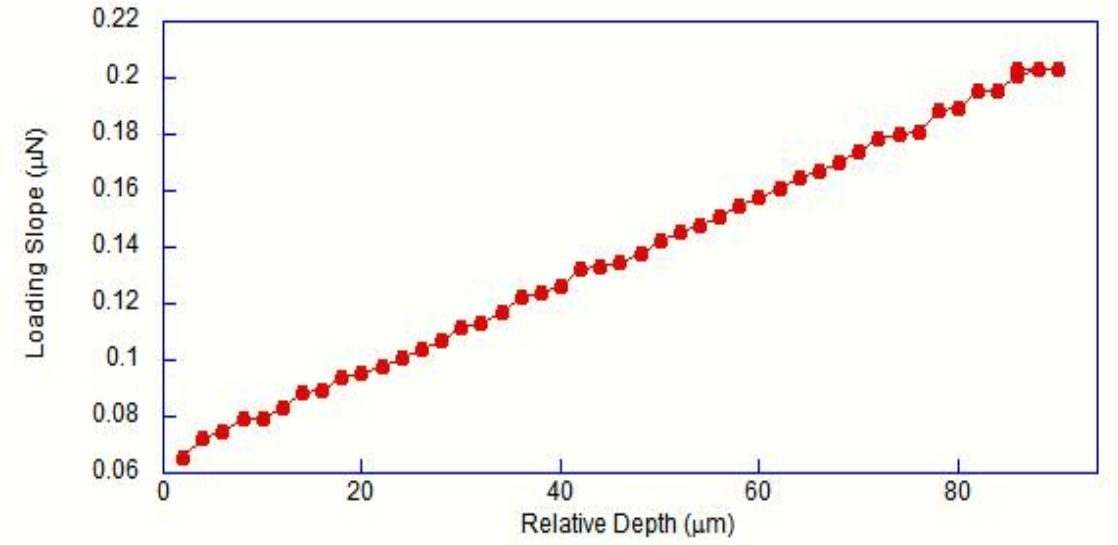

Figure 30. Loading stiffness vs. relative depth (PDMS 50:1).

In Figure 30, it is possible to see that the full contact condition is reached at a relative depth of 88 µm. Table 6 shows the values of the stiffness of the loading slope at every relative depth value. These data are necessary to prove that full contact is reached. The values of the loading slope go from 0.065787 µN/nm during the first indentation, up to 0.20404 µN/n in the 88th indentation. It is possible to see from Table 5 how the value of the loading slope stabilizes once the full contact is obtained.

Table 5. Data collected showing the relative depth and loading slope (PDMS 50:1).

Relative Depth (µm)	Loading Slope (µN/nm)	Relative Depth (µm)	Loading Slope (µN/nm)
2	0.065787	48	0.13781
4	0.072195	50	0.14214
6	0.0747	52	0,14567
8	0.079456	54	0,14765
10	0.079589	56	0,15107
12	0.083416	58	0,15475
14	0.088733	60	0,15739
16	0.089149	62	0,16072
18	0.094068	64	0,1644
20	0.09553	66	0,16705
22	0,098003	68	0,17
24	0,10118	70	0,17372
26	0,10391	72	0,17871
28	0,10717	74	0,17977
30	0,11135	76	0,18101
32	0,11307	78	0,18876
34	0,11674	80	0,18919
36	0,12224	82	0,19552
38	0,12357	84	0,19575
40	0,12599	86	0.19993
42	0,13206	88	0.20302
44	0,13283	86	0.20404
46	0,13497		

Hereafter, the curves at 86 µm, 88 µm, and again 86 µm are studied in order to calculate the elastic modulus of the sample. In Figure 31 these three curves are shown and it is already possible to see how the slope of the aforementioned curves is the same with a reasonably small uncertainty or error in terms of bias and variance.

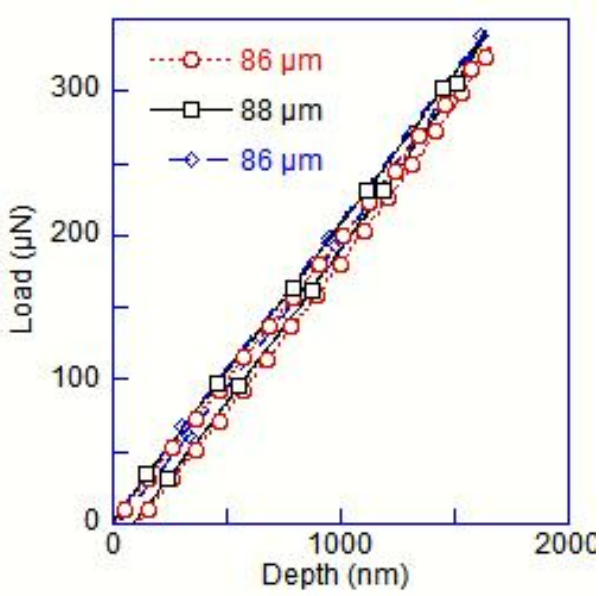

Figure 31. Load-displacement curves after reaching saturation at 100 µm relative tip depth (PDMS 50:1).

The linear fits equations used in this experiment are shown in Figure 32. It is then possible to use the slope of the loading section of the three curves to calculate an average slope.

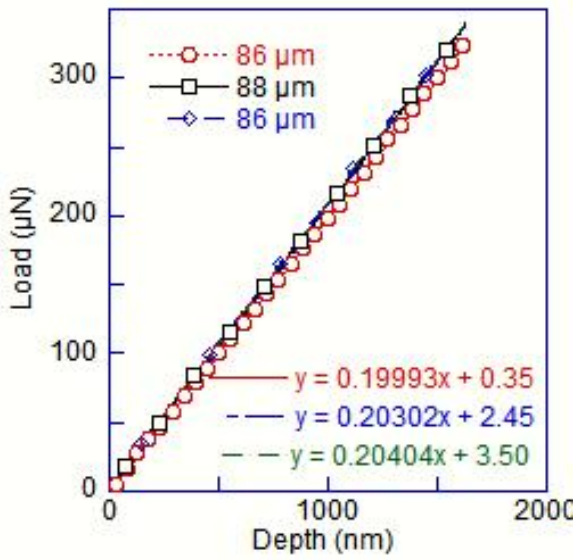

Figure 32. Loading portions of load-displacement curves at 86, 88 and 86 µm relative depth (PDMS 50:1).

First the average slope is calculated using the three fitting equations:

$$y = 0.19993x + 0.35 \tag{27}$$

$$y = 0.20302x + 2.45 \tag{28}$$

$$y = 0.20404x + 3.50 \tag{29}$$

The average slope is then:

$$S_{avg} = \frac{0.19993 + 0.20302 + 0.20404}{3} = 0.2023\ \frac{N}{m} \tag{30}$$

From the equation (6) the reduced elastic modulus is obtained and it is equal to:

$$E_r = \frac{0.2023}{1002.19} = 0.201\ \text{MPa} \pm 0.0021\ \text{MPa} \tag{31}$$

The elastic modulus is then the 75% of the reduced elastic modulus and it is equal to:

$$E = 0.75 * 0.201 = 0.150\ \text{MPa} \tag{32}$$

The elastic modulus of the PDMS sample with a degree of cross-linking 50:1 is then equal to 0.15 MPa or 150 KPa. This value is considered acceptable and it is of the same order of magnitude of the values calculated with different techniques described in the literature. For example, Brown et al. present a result of the elastic modulus of a 50:1 PDMS equal to 90 kPa [51]. In the research of Sharfeddin et al., instead, the values found vary from 0.17 MPa to 0.018 MPa depending if the results are found using a compression or a tensile macro test [50]. However the results available for this cross-linking degree are lacking.

CHAPTER 4: EXPERIMENT TO CALCULATE THE VISCOSITY

4.1 Viscoelasticity

Polymers, such as PDMS, can be classified as solids or viscous fluids and their properties depend on the temperature. If the temperature is low they behave like a rubbery elastic solid or glass, at high temperature, instead, they behave like viscous fluids. At really high temperature, they behave like a liquid with a high level of viscosity. That's why polymers are usually classified as viscoelastic [52]. When a polymer is subjected to a force, the material will react with an instantaneous deformation called elastic deformation and with a time-dependent one called viscoelastic deformation. This kind of deformation is completely recoverable [53]. A viscoelastic behavior is the combination of elastic and viscous behavior.

The model that describes a pure elastic reaction is a spring model and it follows the Hook's law:

$$F_e = K_e e_e \tag{33}$$

where F_e is the force, K_e is the elastic constant of the spring and e_e is the length of the spring [53].

The model that describes the pure viscous reaction is a dashpot model and it follows the equation:

$$F_V = K_V \dot{e_V} \tag{34}$$

where F_V is the force, K_V is the dashpot constant and $\dot{e}_V$ is the change in length of the dashpot [53].

The viscosity is the mathematically defined as the ratio of the shear stress and the strain rate [54]:

$$\eta = \frac{\tau}{\dot{\gamma}} \tag{35}$$

where η is the viscosity, τ is the shear stress and $\dot{\gamma}$ is the strain rate. The units of the shear stress are Pascals (Pa) and of the strain rate are the reciprocal of seconds (s^{-1}). Therefore, the units of the viscosity are Pa*s or Poise (P).

4.2 EVEPVP Model

In the PDMS nanoindentation experiment, the most accurate model is the elastic viscoelastic plastic viscoplastic model (EVEPVP). The schematic model is shown in Figure 10 in chapter 2.3. Mazeran et al. proposed an analytical solution. The model includes a spring to represent the elastic behavior, two Kelvin-Voigt elements for the elasticity comportment, followed by a slider for the plasticity and a dashpot for the viscoplasticity [41].

To calculate the elastic modulus, Mazeran uses the equation (4) presented in chapter 2.2 to obtain the Young's modulus of the tested samples. From the equation (4), the following equation can be derive relationing the load and the displacement graph obtained from the indentation with the elastic modulus:

$$E^* = {k_E}^2 d_E \sqrt{\frac{\pi}{A}} \tag{36}$$

where k_E is the stiffness of the spring and d_E the displacement [41].

For the plastic part, Mazeran et al. used the hardness equation:

$$H = \frac{F}{A} \tag{37}$$

where A is the area of the tip, F the force and H the hardness. From equation (37) the equation relationing the load-displacement graph with the hardness can be derived.

$$H = \frac{p^2 d^2{}_P}{A} \tag{38}$$

where p is the coefficient obtained from the load-displacement graph and $d_P$is the displacement of the plastic element [41].

The viscoelastic part, instead, is modeled with the following equations:

$$E_{VE}{}^* = k_{VE}{}^2 d_{VE} \sqrt{\frac{\pi}{A}} \tag{39}$$

$$\eta_{VE} = 2k_{VE} n_{VE} d_{VE} \sqrt{\frac{\pi}{A}} \tag{40}$$

where k_{VE} is the stiffness, n_{VE} the viscosity and d_{VE} the displacement of the viscoelastic element [41].

For the viscoplastic part, instead, Mazeran et al. used the following model and equations:

$$\eta_{VP} = \frac{n_{VP}{}^2 d_{VP} \dot{d_{VP}}}{A} \tag{41}$$

where n_{VP} is the viscosity and d_{VP} the displacement of the viscoplastic element [41].

4.3 Indentation of 30:1 PDMS Sample

In order to calculate any mechanical property, in this case the viscosity of the sample, the full contact condition has to be reached before proceeding further. In Chapter 3 it is explained how to obtain the full contact. After obtaining full contact, it is then possible to change the function of the application of the force. Viscosity, as stated above, is a time-dependent mechanical property. Because of that, if the loading rate is high enough, there won't be any viscous deformation. During the loading section, if the loading time is small enough, the sample will only be subjected to elastic deformation [55].

In Figure 33, the three different sections of the indentation test are shown: loading section, holding one and unloading section. For this experiment, the loading to the maximum load (equal to 500 µN) is 10 seconds, 60 seconds load holding and 10 seconds for the unloading. A long dwell time has been chosen to minimize the effect of viscosity on the elastic unloading curve [56].

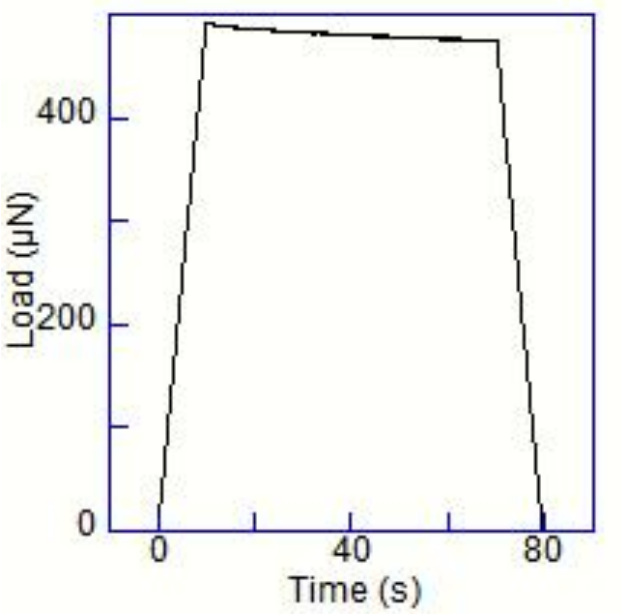

Figure 33. Load-time curve with 10 seconds load and unload and hold of 60 seconds.

The holding time needs to be long enough to allow for viscoelastic deformation. It is then possible to change the holding time to analyze how the sample reacts. In Figure 34 the load-time curves are presented. The graphs represent different indentation tests in which the holding time has been varied from 10 seconds to 600 seconds keeping the loading and unloading time at 10 seconds.

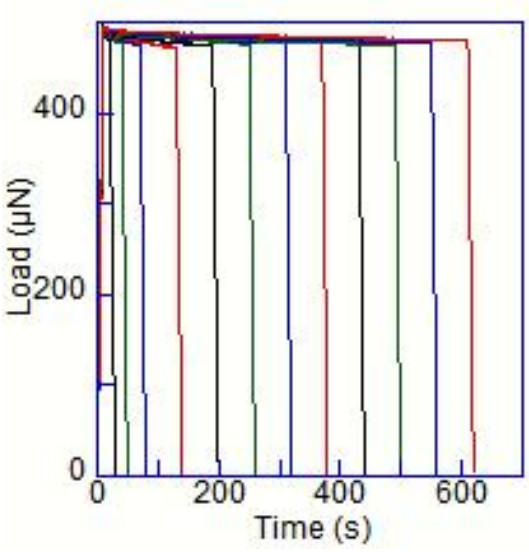

Figure 34. Load-time curves from 10 seconds holding to 600 seconds.

Figure 35 shows more in detail the upper section of the graph shown in Figure 34. That is the most significant segment of the experiment.

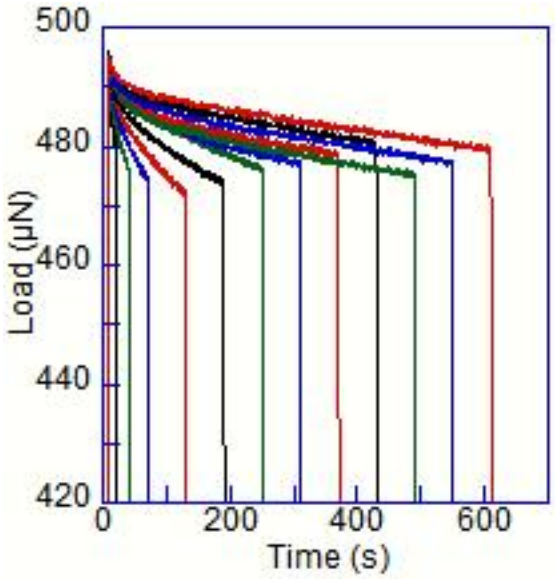

Figure 35. Detail of graph showing the holding time.

Figure 36 shows the load vs depth curves with the holding time that varies from 10 seconds to 600 seconds. When the load force is kept constant, it is possible to see from the graph that the depth will keep increasing [57].

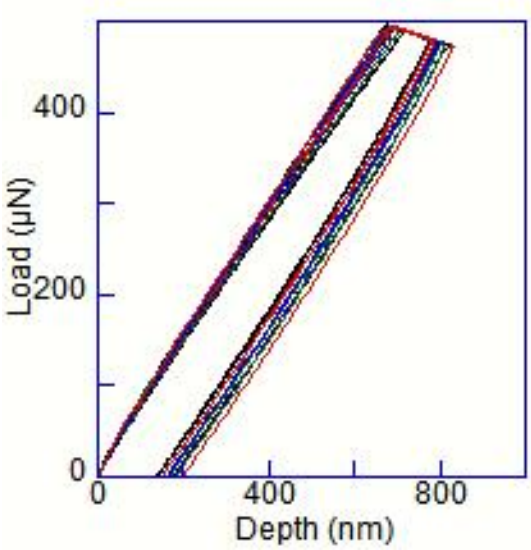

Figure 36. Load-depth graph with different holding times from 10 seconds to 600 seconds.

However, as can be seen in Figure 37, the change in depth during the holding time, decreases with the increasing of the holding time.

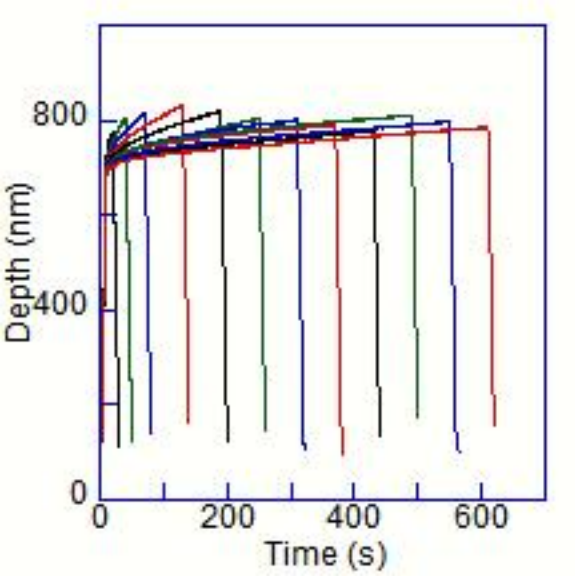

Figure 37. Depth-time curves at different holding times.

Another possible way to analyze the viscoelastic behavior of the PDMS sample is to set the dwell time equal to zero and then change the unloading rate. As said before, the viscous deformation is completely recoverable. In Figure 38 it is possible to see that, even at a very slow unloading rate (up to 1200 seconds) there isn't complete recovery. This happens because it is not a pure viscous deformation.

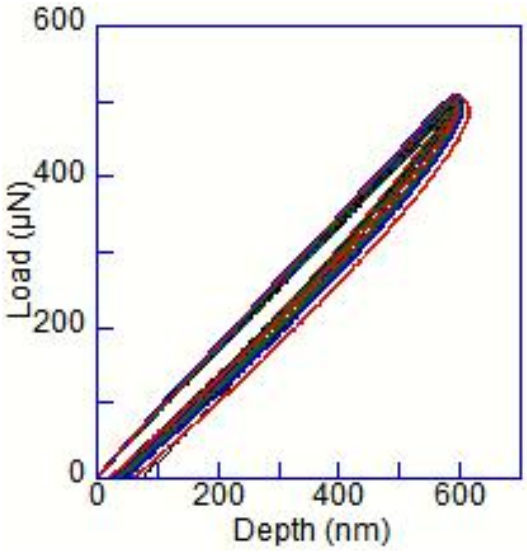

Figure 38. Indentation tests with different unloading rates.

Figure 39 shows more in detail the section of the graph that proves that there isn't full recovery. Even if the time tends to infinite, the $\Delta\delta$ will never reach zero because of the initial load. Zero will only be reached for negative loading values as it can be seen in Figure 40.

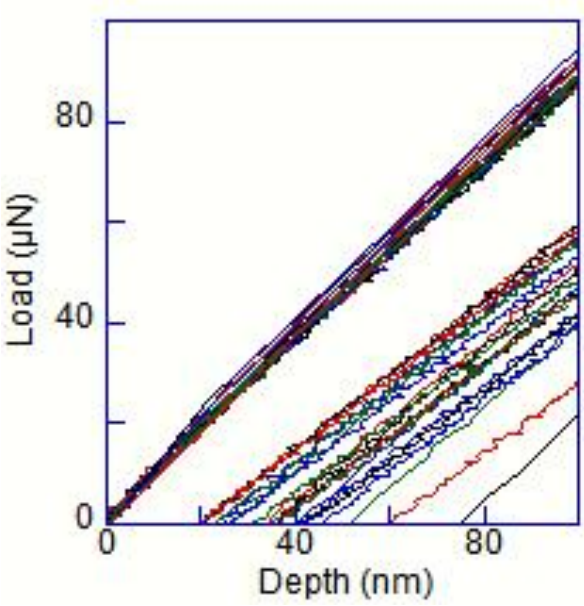

Figure 39. Detail of the load-depth graph with different unloading rates.

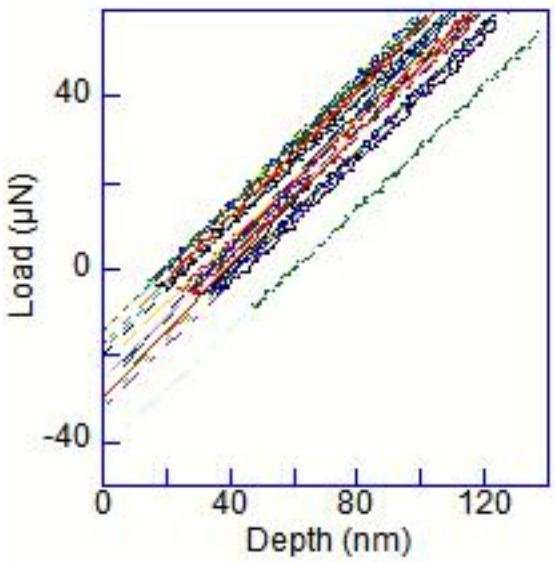

Figure 40. Full recovery for negative load values.

From the graph shown in Figure 39, it is possible to collect some valuable data. Choosing those points where load is equal to 0 N and depth is different from 0 nm, it is possible to find the points of intersection between the curves and the horizontal axis. Those values found represent a change in the displacement ($\Delta\delta$). Figure 41 shows the plot of those values in correlation with the unloading time. This graph represents the progression of post-indentation recovery. In a hypothetical indentation, the full recovery is obtained for load equal to 0 N and change in displacement equal to 0 nm. However, after the unloading, in the experiment is still measured a change in displacement, meaning that there wasn't full recovery [58]. The fact that there isn't full recovery is a direct consequence of the method used to execute the indentation test. The sample of PDMS is always under load even after the end of the unloading. To obtain full contact the sample is already subjected to a load even before the start of the indentation.

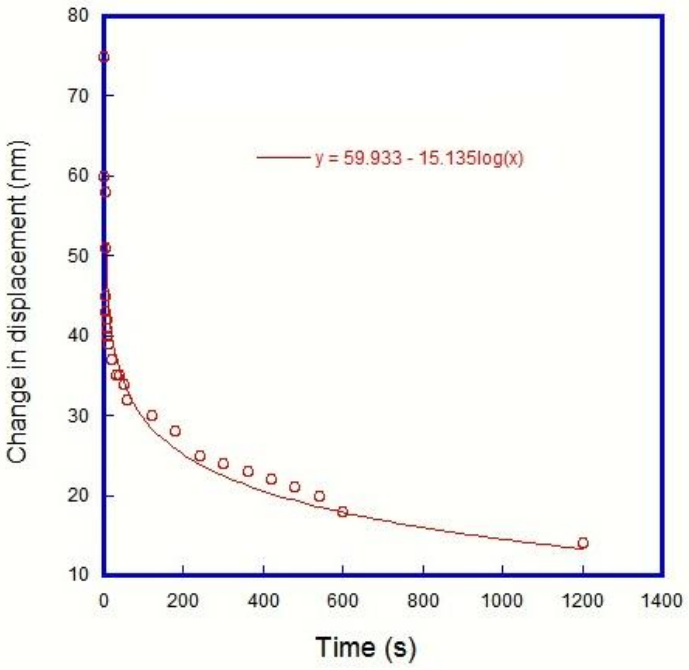

Figure 41. Δδ vs unloading time with logarithmic curve fitting.

Figure 41 shows how the graph stabilizes around a certain value equal to 14 nm. A logarithmic fitting curve describes the trend.

Table 6 shows the obtained data. In order to obtain a more precise value, it would be required to conduct experiments with a smaller increment of the time between two tests in a row.

Table 6. Time of unloading and change in displacement.

Time of unloading (sec)	Δδ Change in displacement (nm)	Time of unloading (sec)	Δδ Change in displacement (nm)
1	75.2	40	35.2
2	60.1	50	34.6
3	58.7	60	32.8
4	51.9	120	30.3
5	45.1	180	28.7
6	43.9	240	25.5
7	42.1	300	24.8
8	41.8	360	23.4
9	40.9	420	22.7
10	39.9	480	21.1
20	37.4	540	20.1
30	35.1	600	18.5
		1200	14.2

The data collected in this section suggest how the viscoelasticity affects the behavior of the PDMS.

The viscosity η can also be defined as the relation between the load and the strain rate:

$$\eta \sim \frac{L}{d\delta/dt} \tag{42}$$

Those values can be extrapolated from the graphs obtained from the nanoindentation. The first experiment analyzed is a test with a holding time relatively small, equal to 120 seconds.

The holding section of the curve needs to be isolated since it is the one used to calculate the values of the variables in the viscosity equation. Figure 42 represents the load versus time graph isolating the holding section of the curve.

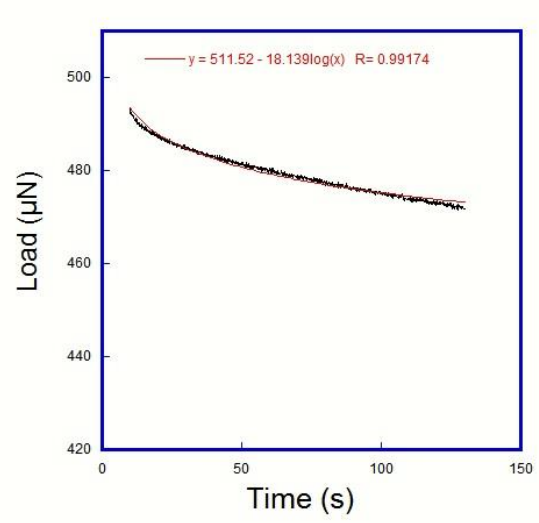

Figure 42. Load vs depth of the holding section of the indentation.

The curve fitting equation that describes the trend of the curve is a logarithmic equation.

To obtain the strain rate from the indentation curve, it is first necessary to isolate the holding section of the displacement versus time graph. The graph is shown in Figure 43. Once again the closest fitting equation to describe the curve is a logarithmic one.

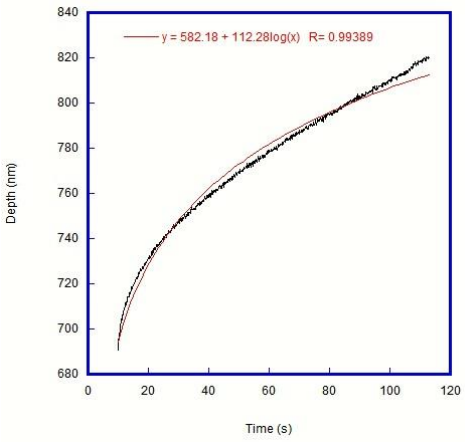

Figure 43. Depth vs time curve of the holding section of the indentation.

The curve fitting equation for the depth versus time curve is:

$$y=582.18+112.28 \log(x) \tag{43}$$

It is then possible to calculate the derivative with respect to the time:

$$\dot{\gamma} = \frac{d\delta}{dt} = \frac{dy}{dx} = \frac{112.28}{x} \tag{44}$$

Once the strain rate is calculated, it is possible to find a numerical value for the strain rate at every time point. To calculate the viscosity at any given time point the load is divided by the stress strain again at every single time point.

After obtaining the values of the viscosity, those results were plotted in the following figures.

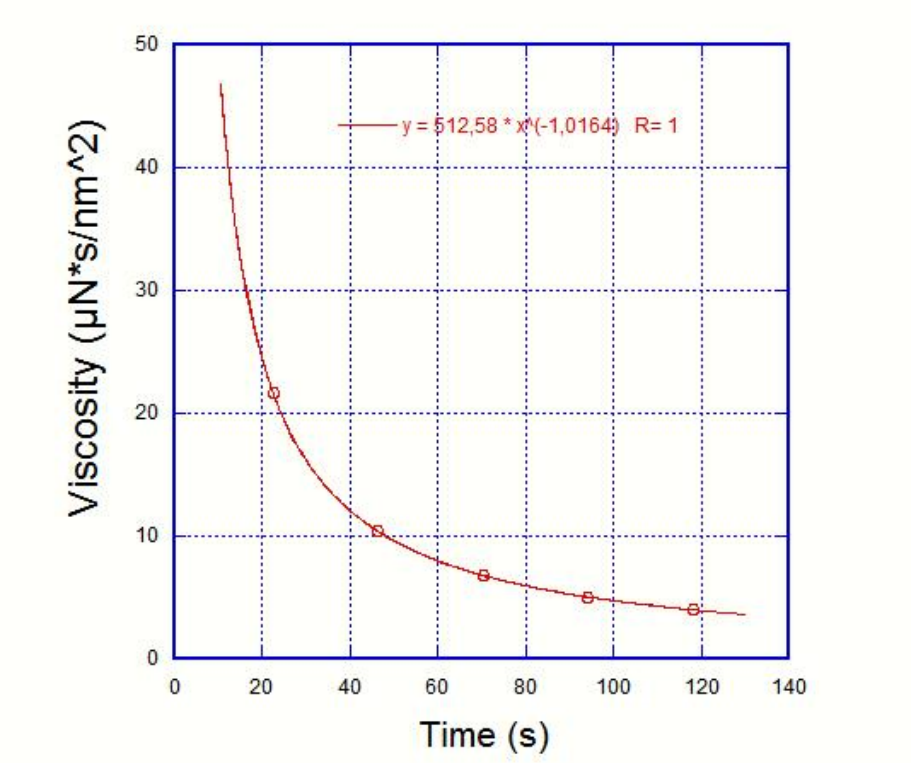

Figure 44. Viscosity vs time.

Figure 44 represents the trend of the viscosity with the time. The only time section that has been kept in consideration is the holding time. It is possible to see how the value of the viscosity rapidly decreases with the time to finally stabilize at a certain value. As described before in this research the holding time needs to be set big enough to minimize the effect of the elasticity. The simplified equation that describes the trend of the viscosity with the time is:

$$\eta = \frac{512.58}{t} \tag{45}$$

Figure 45 represents the trend of the viscosity in comparison with the load. As it can be predicted from the viscosity equation, the viscosity exponentially increases with the increment of the load.

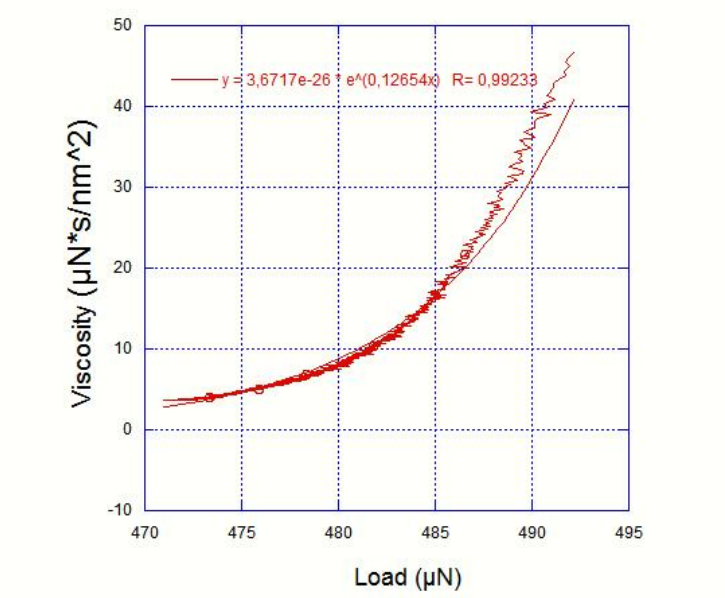

Figure 45. Viscosity vs load.

Another graph that can be obtained is the viscosity versus the depth. Figure 46 shows how the viscosity decreases with the increment of the depth. The curve fitting is an exponential one.

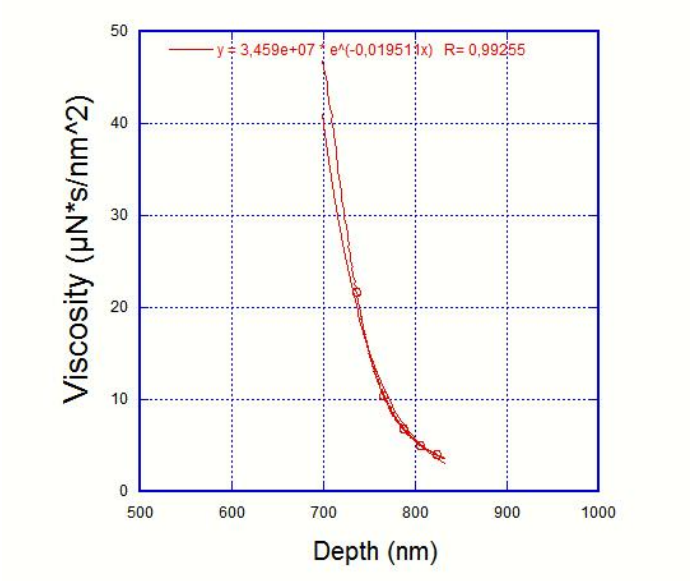

Figure 46. Viscosity vs depth.

However, 120 seconds of holding time is too small to allow to analyze the viscosity without the effect of the elasticity. That's why only the curves with a holding time bigger than 300 seconds have been analyzed to obtain a value for the viscosity.

In Figure 47, it is possible to see how the curve is described by a logarithmic fitting equation for time values smaller than 300 seconds, and as a line for time values bigger than 300 seconds. The only section considered from now on will be the second section were the displacement over the time follows a linear representation.

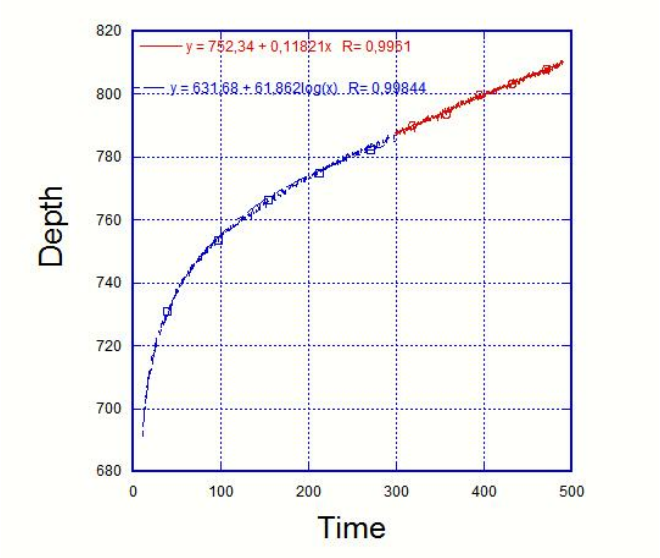

Figure 47. Depth vs time dividing the curve in the two fitting equations.

The indentations that will be analyzed are the ones that present a holding time equal to 360, 420, 480, 540 and 600 seconds.

For each one of these test the following procedure is applied. The first graph, shown in Figure 48, is the load versus time graph. The section kept in consideration is the one where the time is bigger than 300 seconds.

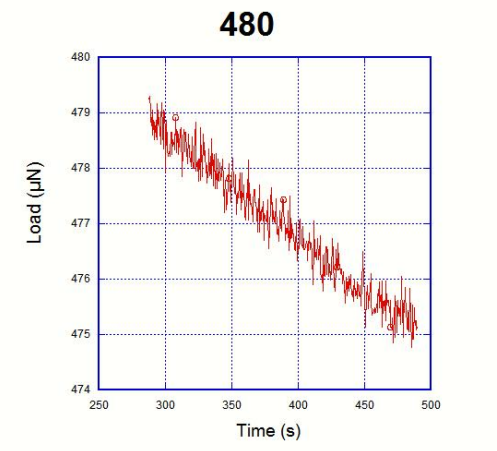

Figure 48. Load vs time for a holding time of 480 seconds.

The second graph, shown in Figure 49, represents the depth versus time of the indentation done with a 480 seconds of holding time. The section of the graph shown is only the one for the time bigger than 300 seconds. A curve fitting equation is extrapolated. The equation represents a line.

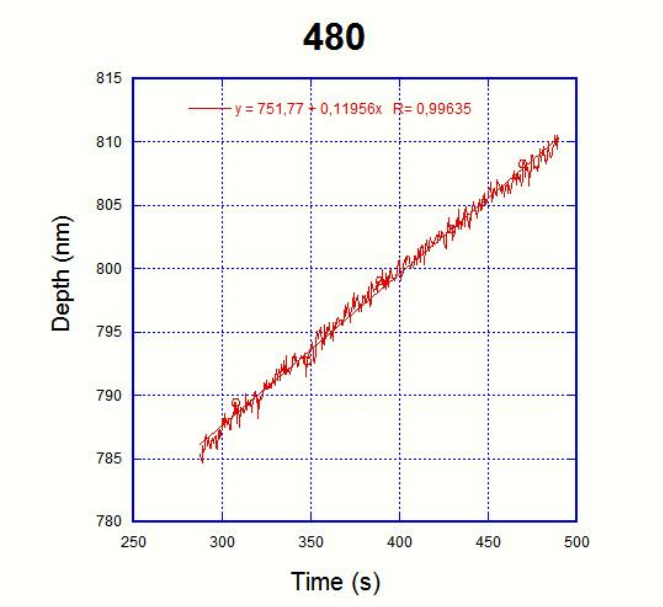

Figure 49. Depth vs time for a holding time of 480 seconds.

The fitting equation is:

$$Y = 751.77 + 0.11956X \tag{46}$$

To calculate the strain rate, the first derivative of the displacement with respect to the time needs to be calculated:

$$\frac{d\delta}{dt} = \frac{dY}{dX} = 0.11956 \tag{47}$$

Once the strain rate has been calculated, it is possible to calculate the viscosity dividing the load by the strain rate. Figure 50 shows the viscosity in relation with the time.

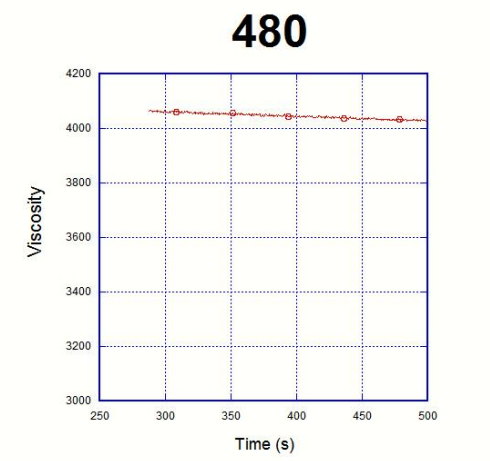

Figure 50. Viscosity vs time for a holding time of 480 seconds.

This procedure can be repeated for every indentation with different holding times. Figure 51 represents all the viscosity results compared with the time. It is possible to see how, for time bigger than 300 seconds, the viscosity is constant and the same for every experiment.

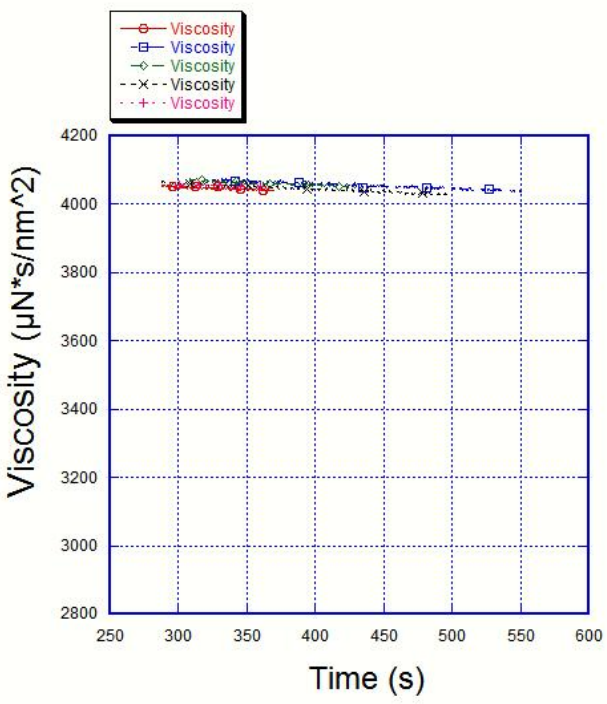

Figure 51. Viscosity vs time for indentations with different holding time.

CHAPTER 5: SUMMARY AND FUTURE WORK

This research has been done in order to deepen the knowledge of PDMS materials through the use of nanoindentation. While macroscopic tests have been widely performed on this kind of material, the micro approach still requires further studies.

The main contribution of this research is the developing of a method to establish full contact between the sample and the tip. The method was then tested on different sample to prove its validity.

Most of the goals set for this research have been reached, however, more experiments can be conducted to prove the results and proceed with the analysis of all the mechanical properties.

In Chapter 1, the objectives of this thesis are exposed after introducing the material studied. Polydimethylsiloxane is described with a chemical and physical approach, as the possible applications are described. After describing the applications, it is obvious why it is of paramount importance to fully understand the behavior and the characteristics of PDMS.

In Chapter 2 the method used to approach this study is introduced. As said before, this thesis only focuses on the study of PDMS through nanoindentation. The instrumentation used is described and the fundamental math, behind it, is presented. To be able to execute the experiments and analyze the results, it is necessary to know the physics of the TriboIndenter and how a nanoindentation works.

In Chapter 3, the main experiment is described and the results are presented. PDMS samples with different cross-linking degrees are tested and the first results shown are from a 10:1 PDMS sample. The full contact method is presented and elastic modulus of the sample is

calculated. The same chapter presents the results obtained applying the same experimental procedure on samples with different cross-linking degrees, such as 30:1 and 50:1.

In Chapter 4, the viscoelasticity is introduced as the mechanical property that is the sum of elastic and viscos behaviors. Fundamental equations of the viscoelasticity are presented and in particular the viscosity is mathematically defined introducing the concept of shear stress and strain rate. The elastic viscoelastic plastic viscoplastic model (EVEPVP) is schematically introduced and the Mazeran's analytical solution is summarized [41]. The same chapter presents the results obtained with the indentation tests and the analysis of the data collected of a 30:1 PDMS sample. Different graphs show the methods to possibly calculate the viscosity of the sample.

Once full contact is assured between the tip and the surface of the sample, it is possible to execute different kinds of tests in order to study different properties or aspects. One of the main goals that should be reached in future research work is the study of the tilt between the tip and the sample and how to calculate and parameterize it. In order to do so, a known tilted tip may be used to calculate the average tilt of the sample. Another possible approach involves a flat punch tip of a smaller diameter. The smaller the diameter is, the less the tilt will influence the results.

Another interesting aspect that needs to be studied more in depth is the aging effect. This is particularly important since PDMS is used for in-body devices and prosthesis such as breast implants. It is needed to study if the aging will cause the change in the mechanical properties of the material [59]. In this research, the samples studied have different ages and it has been shown that stiffness increases with time. However, further studies are needed to prove how the time and the stiffness are related. Samples produced in 2009 and 2015 have been tested.

One of the main reasons why this thesis focused on this material is because of the interested in the application as a substrate for cell growth. Future work will be required to develop technologically advanced microfluidic devices, important to control the chemical environment of the cells [60].

REFERENCES

[1] S.J. Vella, C. Moorlag, Hydrophilic imaging member surface material for variable data ink-based digital printing systems and methods for manufacturing hydrophilic imaging member surface materials, Patent US20150077500 A1 US, March 19, 2015.

[2] Z. Wang, Polydimethylsiloxane mechanical properties measured by macroscopic compression and nanoindentation techniques, Master thesis, 2011.

[3] J. Zhou, D.A. Khodakov, A.V. Ellis, N.H. Voelcker, Surface modification for PDMS-based microfluidic devices, Electrophoresis, 33(1), 89-104, 2012.

[4] E.S. Jung, T.H. Oh, S. Kwon, Micro PDMS hydrogen generator using hydrolysis of sodium borohydride over cobalt nickel-foam catalyst and immobilized cobalt- PH3PO/PDMS/SIO2 catalyst.

[5] T.K. Kim, J.K. Kim, O.C. Jeong, Measurement of nonlinear mechanical properties of PDMS elastomer, Microelectronic Engineering, 88(8), 1982-1985, 2011.

[6] S. Tsvetkov, S. Gateva, M. Taslakov, E. Mariotti and S. Cartaleva1, Light-induced atomic desorption in cells with different PDMS coatings, Journal of Physics: Conference Series, 514, 2014.

[7] T. Dollase, M. Wilhelm, H.W. Spiess, Y. Yagen, R. Yerushalmi-Rozen, M. Gottlieb, Effect of Interfaces on the Crystallization Behavior of PDMS, Interface Science, 11(2), 199-209, 2003.

[8] A.C.M. Kuo, Poly (dimethylsiloxane), Polymer data handbook, 411-435, 1999.

[9] M.J. Owen, Why silicones behave funny, Chemtech, 11(5), 288-292.

[10] A. Vaid, R. Singh, P. Lehana, Developement of microchannel fabrication technique and method to increase trench depth on PDMS.

[11] ChemTube3D.com, The University of Liverpool, 2015.

[12] W. Chen, R.H.W. Lam, J. Fu, Photolithographic surface micromachining of polydimethylsiloxane (PDMS), Lab on a Chip, 12(2), 391-395, 2012.

[13] J.N. Lee, X. Jiang, D. Ryan, G.M. Whitesides, Compatibility of mammalian cells on surfaces of poly (dimethylsiloxane), ,Langmuir, 20(26), 11684-11691, 2004.

[14] A.U. Daniels, Silicone breast implant materials, Swiss Med Wkly 142, w13614, 2012.

[15] T. Fujii, PDMS-based microfluidic devices for biomedical applications, Microelectronic Engineering, 61, 907-914, 2002.

[16] S.H. Im, Shampoo compositions, Wageningen Academic Publishers, Handbook of hair in health and disease, 434-447, 2012.

[17] K. Mojsiewicz-Pieńkowskaa, Z. Jamrógiewicza, J. Łukasiaka, Determination of polydimethylsiloxanes by 1H-NMR in wine and edible oils. Food Additives & Contaminants, 20(5), 438-444, 2003.

[18] M. Andriot, J.V. DeGroot, Jr. and R. Meeks, E. Gerlach, M. Jungk, A.T. Wolf, S. Cray, T. Easton, A. Mountney, S. Leadley, S.H. Chao, A. Colas, F. de Buyl, A. Dupont, J.L. Garaud, F. Gubbels, J.P. Lecomte, B. Lenoble, S. Stassen, C. Stevens, X. Thomas, G. Shearer, Silicones in industrial applications, Silicon-Based Inorganic Polymers, 84, 2009.

[19] A.C.M. Kuo, Silicone Release Coatings for the Pressure Sensitive Industry–Overview and Trends, DC Corporation, 2003.

[20] Z. Wang, A.A. Volinsky, N.D. Gallant, Nanoindentation study of polydimethylsiloxane elastic modulus using Berkovich and flat punch tips, Journal of Applied Polymer Science, 132(5), 2015.

[21] C. Charitidis, Nanoscale deformation and nanomechanical properties of soft matter study cases: polydimethylsiloxane, cells and tissues, International Scholarly Research Notices, 2011.

[22] D.T. Eddington, W.C. Crone, D.J. Beebe, Development of process protocols to fine tune polydimethylsiloxane material properties, 7th International Conference on Miniaturized Chemical and Biochemical Analysis Systems, 2003.

[23] G.C. Lisensky, D.J. Campbell, K.J. Beckman, Replication and compression of surface structures with polydimethylsiloxane elastomer, Journal of Chemical Education 76(4), 537, 1999.

[24] F. Song, D. Ren, Stiffness of cross-linked poly (dimethylsiloxane) affects bacterial adhesion and antibiotic susceptibility of attached cells, Langmuir, 30(34=, 10354-10362, 2014.

[25] M. Liu, J. Sun, Y. Sun, C. Bock, Q. Chen, Thickness-dependent mechanical properties of polydimethylsiloxane membranes, Journal of micromechanics and microengineering 19(3), 035028, 2009.

[26] Z. Wang, A.A. Volinsky, N.D. Gallant, Crosslinking effect on polydimethylsiloxane elastic modulus measured by custom-built compression instrument, Journal of Applied Polymer Science, 131(22), 2014.

[27] A. O'Neill, J.S. Hoo, G. Walker, Rapid curing of PDMS for microfluidic applications, Chips and Tips, 23, 2006.

[28] Corning, Dow. Sylgard 184 Silicone Elastomer. http://www.dowcorning.com/DataFiles/090276fe80190b08.pdf.

[29] R.J.M. Pellenq, A. Kushima, R. Shahsavari, K.J. Van Vliet, M.J. Buehler, S. Yip, F.J. Ulm, Experimental Aspects of Nanoindentation, MIT, Cambridge, Massachusetts : Class Lecture, 10 Feb. 2003

[30] W.A. Bonin, Apparatus for Microindentation Hardness Testing and Surface Imaging Incorporating a Multi-plate Capacitor System. Patent US5553486 A. US, September 10, 1996.

[31] Hysitron. Tip Selection Guide.

[32] Software, TriboScan 9. http://www.hysitron.com/Portals/0/Updated%20Address/TS9XOU%20r1.f.pdf.

[33] S. Bhowmick, S. Asif, O.L. Warren, N. Jaya B, V. Jayaram, S.K. Biswas, In situ SEM Study of Microbeam Bending of Diffusion Aluminide Bond Coats, Microscopy and Microanalysis, 18(S2), 780-781, 2012.

[34] Y.T. Cheng, C.M. Cheng, What is indentation hardness?, Surface and Coatings Technology, 133, 417-424, 2000.

[35] M.A. Dejun, C.W. Ong, L. Jianmin, H.E. Jiawen, Determination of Young's modulus by nanoindentation, Science in China Series E: Technological Sciences, 47(4), 398-408, 2004.

[36] C. Dooley, Analysis of stiffness calculation methods for biomechanical testing when loading and measurement are not coincident spatially, 2012.

[37] J.E. Mark, Polymer data handbook, ed. New York: Oxford university press, 27, 2009.

[38] Y. Zhang, Extracting nanobelt mechanical properties from nanoindentation, Journal of Applied Physics, 107(12), 2010.

[39] S.R. Cohen, E. Kalfon-Cohen, Dynamic nanoindentation by instrumented nanoindentation and force microscopy: a comparative review, Beilstein journal of nanotechnology, 4.1, 815-833, 2013.

[40] Continuum Mechanics SS 2013. Schwarz, Ulrich. Baden-Württemberg, Germany, Heidelberg : Universität Heidelberg, Institut Für Theoretische Physik, 2013.

[41] P.E. Mazeran, M. Beyaoui, M. Bigerelle, Determination of mechanical properties by nanoindentation in the case of viscous materials, International Journal of Materials Research, 103(6), 715-722, 2012.

[42] Standard Linear Model. N.p., n.d. Web. 19 Oct. 2015.

[43] Fischer-Cripps, Methods of Nanoindentation Testing, Introduction to Contact Mechanics, 96-125, 2000.

[44] F. De Paoli, A.A. Volinsky, Obtaining full contact for measuring polydimethylsiloxane mechanical properties with flat punch nanoindentation, MethodsX, accepted 2015, DOI: 10.1016/j.mex.2015.09.004

[45] Triboindenter User Manual, Hysitron Inc. (2003).

[46] Contributors, Wikipedia. Stress–strain curve. [Online] Wikipedia, The Free Encyclopedia., 06 02, 2015. [Cited: 06 05, 2015.] http://en.wikipedia.org/w/index.php?title=Stress%E2%80%93strain_curve&oldid=665176743.

[47] J.Y. Sun, J. Tong, Z.J. Zhang, The specimen preparation methods for nanoindentation testing of biomaterials: a review, International Society for Optics and Photonics, In Photonics Asia, 2007.

[48] S. Gupta, Analytical and numerical nanoindentation studies of compliant biomaterials and soft tissues, ProQuest, 2008.

[49] G.G. Genchi, G. Ciofani, I. Liakos, L. Ricotti, Bio/non-bio interfaces: a straightforward method for obtaining long term PDMS/muscle cell biohybrid constructs, Colloids and Surfaces B: Biointerfaces, 105, 144-151, 2013.

[50] A. Sharfeddin, A.A. Volinsky, G. Mohan, N.D. Gallant, Comparison of the macroscale and microscale tests for measuring elastic properties of polydimethylsiloxane, Journal of Applied Polymer Science, 132(42), 2015.

[51] X.Q. Brown, K. Ookawa, J.Y. Wong, Evaluation of polydimethylsiloxane scaffolds with physiologically-relevant elastic moduli: interplay of substrate mechanics and surface chemistry effects on vascular smooth muscle cell response, Biomaterials, 26(16), 3123-3129, 2005.

[52] Visco-Elasticità, Retrieved September 2, 2015, from climeg.poliba.it/mod/resource/view.php?id=1657

[53] W.F. Hosford, Mechanical behavior of materials, Cambridge University Press, 2010.

[54] M. Fincan, Assessing Viscoelastic Properties of Polydimethylsiloxane (PDMS) Using Loading and Unloading of the Macroscopic Compression Test. Diss. University of South Florida, 2015.

[55] S.J. Yang, K. Jiang, Elastomer Application in Microsystem and Microfluidics, 2012.

[56] T. Sveaass, Nano-Indentation of Anisotropic Material: Numerical Approaches to Extract Elasticities from Nano-Indentation, 2013.

[57] B.J. Briscoe, L. Fiori, E. Pelillo, Nano-indentation of polymeric surfaces, Journal of Physics D: Applied Physics, 31(19), 2395, 1998.

[58] C.A. Tweedie, K.J. Van Vliet, On the indentation recovery and fleeting hardness of polymers, Journal of materials research, 21(12), 3029-3036, 2006.

[59] A.B. Birkefeld, H. Eckert, B. Pfleiderer, A study of the aging of silicone breast implants using 29 Si, 1 H relaxation and DSC measurements, Biomaterials, 25(18), 4405-4413, 2004.

[60] J.M. Dechene, Surface Modifications of Poly (dimethylsiloxane) for Biological Application of Microfluidic Devices, 2010.

APPENDIX A: TRIBOINDENTER CALIBRATION PROCEDURE

The following are the setup values and procedure used to execute the calibration of the TriboIndenter. The calibration will consist of repeating an air indentation twice.

To obtain a valid calibration, the values of the control knobs on the TriboIndenter and on the software need to be set up as described:

- the low pass filter needs to be set at 300 Hz;
- the Displacement Gain and the Microscope Feedback Gain have to be set at 100;
- The Bias needs to be switched to "ON" in the Triboscan software.

To start the test of the sample, it is necessary to define a workspace. This workspace needs to be defined at a Z-level lower than the real height of the sample to avoid the retraction of the tip after each indentation. It is important to remember that, while the relative movement of the tip takes place, the machine needs to be re-zeroed pressing the auto zero button on the lower part of the TriboIndenter. It is important to re-zero at the exact moment when the Z motors are ON or an error will occur and the motors will be stopped and the tip retracted. It is possible to see when the Z motors are ON because the light on the lower part of the machine, relative to the Z axis, will turn green instead of yellow.

APPENDIX B: SAMPLE PREPARATION STEP BY STEP

In this appendix the technique how to create PDMS samples is shown. It involves the following steps:

1. Placing the cup on the digital analytical balance and taring it, as shown in Figure B.1.

Figure B.1. Digital analytic balance.

2. Pouring the Sylgard 184 silicone elastomer base in the cup and taring the balance again. Figure B.2 shows the adding of silicone elastomer curing agent. This is how the cross-linking degree will be defined.

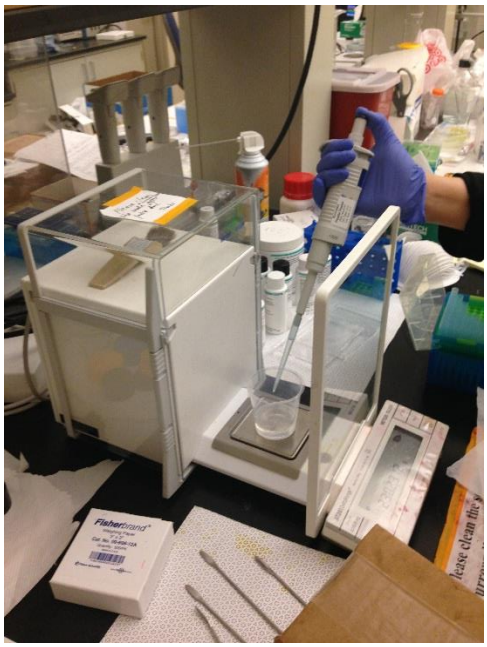

Figure B.2. Adding Sylgard 184 curing agent.

In this procedure, the production of a PDMS 10:1 is described. For every 10 grams of base, 1 gram of silicone curing agent will be poured into the cup. To keep a satisfying level of precision, a Pasteur pipette can be used to complete this step.

3. Mixing the composite with a spoon in order to spread, homogeneously, the curing agent in the base. For samples 10:1 or 30:1, the mixing time required is around 15 minutes. For samples with a lower degree of cross-linking, such as 50:1, around 30 minutes are required. One factor that is important during the mixing process is the speed kept during the procedure. It is appropriate to keep a constant speed.
4. Putting the cup filled with the mixture in the vacuum desiccator (Figure B.3) to make all the bubbles disappear from the composite. The sample needs to be kept in the desiccator for around 30 minutes. The time needed to eliminate all the bubbles is positively related to the time of mixing. Figure B.4 shows an intermediate condition. The mixture vacuumed for 15 minutes still presents bubbles.

Figure B.3. Vacuum desiccator used to eliminate bubbles.

Figure B.4. Intermediate condition after 15 minutes of vacuuming.

5. Pouring the PDMS on a Petri dish, avoiding any bubble formation. In case of bubbles formation, it is possible to poke the bubbles with a needle to release the air.

6. At this point, the sample is almost ready. It needs time to cure. This procedure can be done at the room temperature or with the use of an oven. Using an oven the time necessary to cure the sample will be significantly less. Figure B.5 shows the oven used in this experiment set at a temperature of 65 °C.

Figure B.5. Oven used to cure the samples.

APPENDIX C: COPYRIGHT PERMISSIONS

The permission below is for material in Chapter 3.

MethodsX aims at having a transparent and quick editorial process. All submitted articles conform to the *MethodsX* format will be sent out for review. As the content of a *MethodsX* article is purely technical, reviewers are asked to focus on the technical aspects of the manuscript. Are the procedures suggested by the authors plausible? Are the methods clear and logical to follow, so that someone else could reproduce them easily?

View the full set of Reviewer Guidelines here

Authors are invited to revise and resubmit their manuscript when reviews are overall positive and request textual adjustments only. If extensive additional experiments are required, authors will be advised that their manuscript cannot be accepted for publication. Of course, every author will be welcome to resubmit their manuscript anew in the future.
MethodsX is a community effort, by researchers for researchers. We appreciate the work not only of the authors submitting, but also of the reviewers who provide valuable input to each submission. We therefore publish a standard "reviewer thank you" note in each published article and give the reviewers the choice to be named or to remain anonymous.

When submitting, **please provide a minimum of three suitable potential reviewers** (including their name, institutional email addresses, and institutional affiliation). When compiling this list of potential reviewers please consider the following important criteria: they must be knowledgeable about the manuscript subject area; must not be from your own institution; at least two of the suggested reviewers should be from another country than the authors'; and they should not have recent (less than four years) joint publications with any of the authors. However, the final choice of reviewers is at the editors' discretion.

Please note that **no cover letter to the Editor is required**. Should you have comments or questions to the Editor, you can submit them in a free text box in the course of the submission process (submission step entitled Enter Comments).

Open access and Copyright

This journal is fully open access; all articles will be immediately and permanently free for everyone to read and download. Upon acceptance of an article, authors will be asked to complete an 'Exclusive License Agreement' where authors will retain copyright (for more information on this see http://www.elsevier.com/OAauthoragreement.) Permitted reuse is defined by the following Creative Commons user license:

Creative Commons Attribution (CC BY): lets others distribute and copy the article, to create extracts, abstracts, and other revised versions, adaptations or derivative works of or from an article (such as a translation), to include in a collective work (such as an anthology), to text or data mine the article, even for commercial purposes, as long as they credit the author(s), do not represent the author as endorsing their adaptation of the article, and do not modify the article in such a way as to damage the author's honor or reputation.